DEVELOPING A SOIL PROPERTY DATABASE FOR THE OKLAHOMA MESONET

By

BETHANY SCOTT

Bachelor of Science in Environmental Science

Oklahoma State University

Stillwater, OK

2010

Submitted to the Faculty of the
Graduate College of the
Oklahoma State University
in partial fulfillment of
the requirements for
the Degree of
MASTER OF SCIENCE
December, 2012

DEVELOPING A SOIL PROPERTY DATABASE FOR THE OKLAHOMA MESONET

Thesis Approved:

Dr. Tyson Ochsner

Thesis Adviser

Dr. Brian Carter

Dr. Todd Halihan

Dr. Sheryl A. Tucker

Dean of the Graduate College

ACKNOWLEGMENTS

I would like to sincerely thank my advisor for being ever patient and knowledgeable during this rewarding journey. I would also like to acknowledge all of the undergraduate research assistants who have played such a large role in this project including Sam Wallace, Thomas Hyde, Michelle Melone, and Jordan Beehler as well as my Soil Physics colleges, Geano Dong, Yohannes Yimam, and Navneet Bilga. Finally, thank you to my loving spouse, Franklin Scott for cheering me on during all the late nights.

Acknowledgements reflect the views of the author and are not endorsed by committee members or Oklahoma State University.

TABLE OF CONTENTS

LIST OF TABLES

Table Page

LIST OF FIGURES

Figure Page

CHAPTER I

INTRODUCTION

1.1 The Oklahoma Mesonet. In 1994, as a joint project between Oklahoma State University and the University of Oklahoma, the environmental monitoring system of the Oklahoma Mesonet was established. The Mesonet consists of 120 stations with at least one station in each of Oklahoma's 77 counties. Average station spacing is 50 km, which encompasses the medium, or meso, scale of variability found in many environmental variables (McPherson et al., 2007). Over 20 environmental variables are monitored at each station with readings taken at 5 to 30 minute intervals (Brock et al., 1995). Beginning in 1996, the CSI 229-L heat dissipation sensor was installed at a majority of the sites to monitor soil matric potential with sensors at 5, 25, and 60 cm depths with readings available every 30 minutes (Illston et al., 2008) Detailed descriptions of the site design, data quality and control, and data acquisition for the Oklahoma Mesonet have already been completed and can be found by Brock et al., (1995), Illston and Basara (2008), and on the system website, www.mesonet.org , respectively.

The comprehensive dataset of soil matric potential readings spanning nearly 16 years, is often used by researchers in hydrology and related disciplines for studies of soil water content spatial and temporal variability (DeLiberty and Legates, 2008; DeLiberty and Legates, 2003), land atmosphere interaction (Godfrey and Stensrud, 2008), groundwater storage estimation (Swenson et al., 2008), and soil water content remote

sensing validation (Holmes et al., 2012). However, the estimated accuracy of the Mesonet soil water content data is ±0.066 cm^3 cm^{-3} (Illston et al., 2008), which is not adequate to meet requirements of some applications. For example, contemporary satellite missions (e.g. SMOS, SMAP) aim to provide surface soil moisture measurements with accuracy of ±0.04 cm^3 cm^{-3} (Kerr et al., 2001). Furthermore, direct measurement of many of the properties that control soil hydrology including field capacity (FC) and permanent wilting point (PWP) have not been completed for a majority of the Mesonet Stations. This deficiency limits the use of Mesonet data in research as well as in applied purposes like drought monitoring. Plant available water (PAW), an effective drought indicator, quantifies available soil moisture on a depth basis resulting in output that is readily understandable and applicable. In order to calculate PAW, key soil physical properties must be known. A comprehensive database that includes direct measurements of soil physical properties is needed to improve the accuracy and applicability of a major environmental monitoring system, the Oklahoma Mesonet.

1.2 Soil Moisture Monitoring.

1.2.1. Sensors. The CSI 229-L heat dissipation sensor consists of a heating element and thermocouple placed in epoxy in a hypodermic needle, which is encased in a porous ceramic matrix. A current is applied to the heating element for 21 seconds, after which the thermocouple measures the temperature rise. The amount of water in the porous ceramic matrix changes as the surrounding soil wets and dries, which effects the magnitude of the temperature rise, ΔT, that is observed (Flint et al., 2002). The temperature rise is then normalized using sensor specific calibration coefficients and

represented as ΔT_{ref} to account for sensor to sensor variation (Illston et al., 2008). Soil matric potential is then calculated using Eq. [1].

$$\psi_m = -c * \exp(a\Delta T) \quad \textbf{[1]}$$

where ψ_m is the matric potential (kPa), ΔT is the temperature change and sensor output (°C), and c and a are calibration constants equal to 0.717 kPa and 1.7880 $°C^{-1}$, respectively (Illston et al., 2008).

1.2.2. Pedo-transfer function. The matric potential can be converted to soil water content based on the site and depth specific water retention curve (WRC). The combination of particle size distribution along with bulk density is often used to predict soil water retention and hydraulic conductivity functions (Mohanty et al., 2002). These prediction models are called pedo-transfer functions (PTFs). Several forms exits including a simple look up table based on textural class such as the ARS USDA Rosetta class average look up table (Schaap et al., 2001a), the Arya and Paris method (Arya and Paris, 1981) which uses a detailed particle size distribution along with the bulk density, and the neural network model Rosetta, used to model the drying water retention curve (Schaap et al., 2001a).

The matric potential value from the 229-L Mesonet sensors was previously converted to soil water content based on the site and depth specific water retention curve estimated from particle-size distribution and bulk density using the PTF developed by Arya and Paris (1981). This method does not take into account soil structure; methods failing to account for structure can lead to significant error in medium and fine texture soils in which the WRC is highly influenced by soil structure (Hillel, 2004). The current

method resulted in a root mean squared difference (RMSD), or deviation from the 1:1 line, of 0.066 cm^3cm^{-3} when volumetric water content estimates based on the 229-L sensor data were compared to direct measurements made by oven- drying (Illston et al.,2008). Vereecken et al. (2010) outlines the importance of continued development of PTFs through the "establishment of databases of soil hydraulic properties that are derived from standardized measurement procedures, and contain predictors of soil structure." In order to improve the estimation of soil water content by the Mesonet, the establishment of a soil hydraulic properties database, combined with a PTF which considers soil structure, is crucial.

One of the most widely-used PTFs to date is the artificial neural network (ANN) model, Rosetta (Schaap *et al.,* 1998). The Rosetta model takes soil structure in to account through the input of soil water content at -33 kPa. Rosetta is an ANN for estimating the parameters of the water retention curve of van Genuchten (1980). The advantage to using an ANN compared to traditional PTFs is that ANNs do not require a prior model concept. Therefore, the optimal relationship between input and output data is obtained through the calibration process (Schaap *et al.*, 1998). Rosetta utilizes a hierarchical structure that allows input of 1-5 predictors, with accuracy increasing with the number of predictors. The Rosetta neural network approach has been found to significantly reduce error associated with hydraulic property estimation. Schaap et al. (2001a) evaluated the root mean square error between measured and estimated water contents and found that the error decreased with the ANN method versus traditional PTFs as well as decreasing with increased number of input parameters in Rosetta from 0.078 $cm^3\ cm^{-3}$ with only the textural class as an input to 0.044 $cm^3\ cm^{-3}$ with five inputs. The five inputs required for

this increase in accuracy in Rosetta include the percent sand, silt, and clay, the bulk density, and the water content at -33 and -1500 kPa, which correspond to the field capacity and permanent wilting point of the soil. Because of its ease of use, options in input, and demonstrated accuracy (Schaap et al., 2004), Rosetta was selected in this study to estimate the water retention curve parameters of soil samples obtained from the Oklahoma Mesonet stations.

The hydraulic parameters Rosetta estimates are from the van Genuchten equation shown here as Eq. [2] (van Genuchten, 1980).

$$\frac{\theta - \theta_r}{\theta_s - \theta_r} = \left[\frac{1}{1 + (-\alpha \psi_m)^n} \right]^m \quad \textbf{[2]}$$

The parameters include θ_r (cm^3 cm^{-3}), which is the residual volumetric water content (at high suction), θ_s (cm^3 cm^{-3}) which is the saturated volumetric water content, α is a fitting parameter inversely related the air entry suction, n is a fitting parameter which affects the shape of the curve and m (-), a fitting parameter represented as $m = 1 - 1/n$ (Schaap et al., 2001a). Theses parameters are then used to calculate the current volumetric water content, θ, given the soil matric potential, ψ_m, measured by the Mesonet sensors. In addition, Rosetta models the saturated hydraulic conductivity, K_s, as Eq. [3]

$$Ks = K_o S_e^L \{1 - \left[1 - S_e^{\frac{n}{n-1}}\right]^{1-\frac{1}{n}}\}^2 \quad \textbf{[3]}$$

where K_o (cm day^{-1}) is a fitted matching point at saturation, L (-) is an empirical parameter, and S_e (-) is the effective saturation (Schaap et al., 2001a).

1.2.3. Plant available water. Improved estimates of the soil water retention properties at the Mesonet sites will create opportunities for studying not just soil water content but also plant available water (PAW). Plant available water is defined as the amount of water stored in the soil profile above the permanent wilting point, estimated at -1500 kPa (Brady and Weil, 1999). Different soil textures will loose and retain water at different rates, making estimation based on detailed soil characterization important. Point measurements of PAW at each of the Mesonet stations have value, but maps produced by spatial interpolation of PAW allows visualization of patterns to facilitate decisions made by end users of Mesonet data.

1.3. Spatial Interpolation. Soil water content varies at multiple scales in space and time and is an important component of the energy and water cycle because it controls interactions between the land surface and the atmosphere (DeLiberty and Legates, 2008). Researchers have proposed that the spatial variation of soil water content consists of a smaller land surface scale and larger atmospheric scale. The smaller land surface scale is related to soil and topographic variability and hydrologic processes and varies on the scale of tens of meters; whereas the atmospheric variability is on a scale of several hundred kilometers (Vinnikov *et al.*, 1996). Oklahoma Mesonet stations are approximately 50 km apart, making the interpolation based on large or atmospheric scale variability feasible.

Many studies have investigated the spatial and temporal variability of soil moisture (Brocca et al., 2012; Choi et al., 2007; Illston et al., 2004; Lakhankar et al., 2010). However, very few studies have looked at the large scale spatial patterns of soil water content through mapping monitoring network data and no published studies are

available on the spatial structure of PAW, most studies have focused instead on models or satellite data of soil moisture. However, kriging has been used successfully in a recent study by Lakhankar et al. (2010) to interpolate Mesonet soil water content data. Lakhankar et al. established a semivariogram for soil water content during their study. They found the semivariogram range is 175 km, meaning that the semivariance reaches a maximum at that distance; the nugget or initial rise, shows the small scale variation in samples that are close together. They found that large-scale spatial patterns account for approximately 66% of the spatial variance of soil water content in Oklahoma. The new soil property database combined with the Mesonet sensor network creates powerful new opportunities to study the spatial variability of soil moisture.

1.4. Objective statement and thesis organization. This study differs from and expands on the existing studies of soil moisture networks in two important ways; (i) by improving the accuracy of the modeled hydraulic parameters through detailed physical and hydraulic property characterization at each Mesonet station, (ii) by development of PAW maps, currently available on the Oklahoma Mesonet website. The main objective of this research is to provide increased accuracy for the Mesonet soil water content data through improved estimates of water retention curve parameters enabled by a comprehensive new database of soil hydraulic and physical properties of the Oklahoma Mesonet station soils.

Chapter 2 provides detailed descriptions of the sampling area and plan, lab procedures and database design. Chapter 3 describes the improved accuracy of Mesonet soil water content resulting from the new database along with other possible applications for the database, including maps of PAW based on kriging. Chapter four outlines possible sources of improvement and future research considerations.

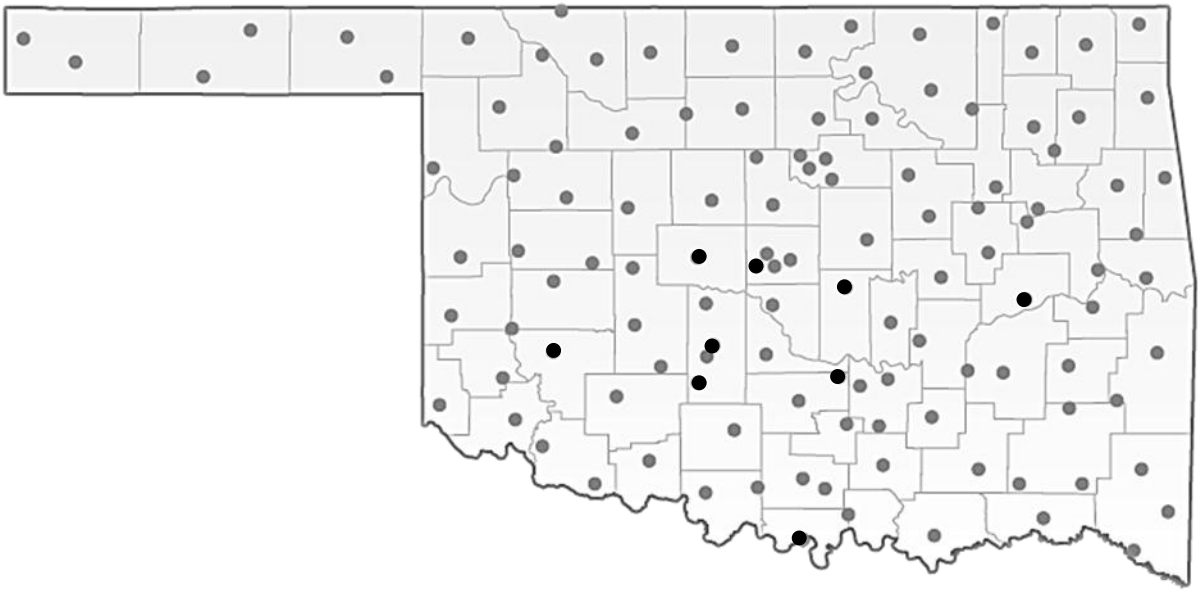

Figure 1.1 Map of the Oklahoma Mesonet station locations (●) with validation sites indicated (●)

CHAPTER II

MATERIAL AND METHODS

2.1 Study Area and Sampling Plan. The study area encompassed the entire state of Oklahoma. Located in the Southern Great Plains, the topography varies from nearly flat in the west to rolling plains in the northeastern Ozark Plateau. Vegetation types vary from predominantly grasslands to mixed hardwood forests. Climate variation is pronounced with a humid subtropical climate in the east transitioning to semi-arid in the west with a sharp decrease in precipitation from the southeast corner where it averages 142 cm per year, to the northwest panhandle, with 43 cm per year. Extreme temperature variability exists with temperatures above 32° C occurring 60-65 days a year and temperatures of 0° C or less occurring on average 60 days a year. Severe weather outbreaks include flooding, tornadoes, severe thunderstorms, and severe drought. (Arndt, 1997).

Soil core samples were collected April-August of 2009 and 2010 at 117 of the 120 Oklahoma Mesonet stations. A Giddings hydraulic soil sampler, model 15-SC/ GSRPS, (Baarstad *et al.*, 1992) was used to extract two replicate cores within a maximum distance of 3 m from the soil water content sensors. Cores were collected using an 8.9 cm diameter steel tube to a depth of 80 cm or to the depth of bedrock. Care was taken to minimize effects to the stations by backfilling all core sites with sand. Core integrity was determined by comparing the length of the core to the depth of the bore hole; only samples that had greater than 90% agreement were accepted.

2.2 Core Sections. Each core was sectioned into 3-10, 20-30, 40-50, 55-65, and 70-80 cm intervals on site. The top 3 cm section of the cores were discarded due to thick grass roots which prevent accurate measurements (Mohanty et al., 2002). Each interval is centered on the depth of existing Mesonet 229-L sensors excluding the 40-50 cm interval which a candidate depth for future sensor installation. The 70-80 cm interval sensors were decommissioned by the Mesonet in January of 2011; however archive data will remain available. Each core section was sealed in a plastic bag and placed in a cooler to minimize water loss from the samples during transport to the laboratory. All samples were weighed and placed in the laboratory controlled humidity and temperature room at 5°C within 24 hours of collection.

2.3 Volumetric water content at sampling. The volumetric water content at field conditions was calculated from the gravimetric water content found through oven drying a subsample of each core section multiplied by the bulk density determined from the total core section volume and dry mass (Topp and Ferre', 2002). Samples were weighed before and after being dried at 105° C. The volumetric water content was calculated from the daily average ΔT_{ref} output from the Oklahoma Mesonet 229-L heat dissipation sensors on the day each site was sampled. The ΔT_{ref} values were converted to ψ_m by Eq. [1] and then to volumetric water content by Eq. [2] using the parameters in the new database. Uncertainty in the soil water content due to small scale spatial variations and the unavoidable distance (2-3 m) between soil cores and the in situ sensors was estimated based on the RMSD between water contents from replicate soil cores for each site and depth combination.

2.4 Bulk density. An adapted version of the core method (Grossman and Reinsch, 2002) was used to determine the bulk density of the samples. The resulting bulk density represents that of the soil matrix only. A subsample of the core section was used to determine the rock fraction, or percentage of particles larger than 2 mm, present in the larger sample. The subsample was dried at 105° C, ground using a hammer mill and, if necessary, a mortar and pestle, and then sieved through a 2 mm sieve. The mass of the rocks in the subsample was then determined. The ratio of that mass to the dry mass of the subsample provided an estimate of the rock fraction, RF. The rock fraction was then applied to Eq. [4] to determine bulk density, ρ_b, of the soil matrix.

$$\rho_b = \frac{m_d*(1-RF)}{V-RF*m_d/\rho_R} \quad \textbf{[4]}$$

where m_d (g) is the mass of the dry core section including rocks, V (cm^3) is the volume of the core section, and ρ_R (g cm^{-3}) is the density of rock. A rock bulk density of 2.6 g cm^{-3} was used because it is the average of shale and sandstone, two of the most common rock parent materials found in Oklahoma (Johnson, 2008). A total of four samples had large rocks that prevented subsampling. For these samples, the entire section was used as opposed to a subsample. The section was dried, separated, and the rock fraction determined as in Eq. [4]. A total of 7.4 percent of the samples contained a rock fraction of 5 percent or greater. This method was used, as opposed to a more rigorous method for estimating rock fraction, due to the extensive area covered by the sampling plan, as well as the destructiveness of collecting samples large enough to accurately represent the bulk density of the soil with rocks present. The bulk density data were analyzed for quality control by removing outliers from the data set. Outliers were determined as values that

were 2 times the interquartile range (IQR) below the first quartile or above the third quartile.

2.5 Water content at -33 and -1500 kPa. All gravimetric water content values were converted to volumetric water content using the determined bulk density. Field capacity was approximated by the amount of water remaining in the soil after equilibration at –33 kPa by the pressure cell (Tempe cell) method (Dane and Hopmans, 2002). The intact core sections were trimmed to a height of ~4 cm and sealed with wax to fill the annular gap between the 8.9 cm pressure cell ring and the 7.5 cm sample (Ahuja *et al.*, 1985). The permanent wilting point (PWP), defined as the soil water content at which plants wilt and cannot recover, was approximated in the laboratory by pressure plate extraction at -1500 kPa (Dane and Hopmans, 2002). Pressure plate extraction was performed using a subsample of each core section that had been dried at 105°C and ground to pass a 2 mm sieve.

The water content at -33 kPa and -1500 kPa data were analyzed for quality control by removing outliers from the data set. Outliers were determined as values that were 1.5 times the IQR below the first quartile or above the third quartile. The available water capacity, or the water between -33 and -1500 kPa, was calculated and if the result was negative both water retention measurements were removed from the dataset.

2.6 Particle size distribution. The textural class of each sample was determined based on the percent sand, silt, and clay measured using the hydrometer method outlined by Gavlak et al. (2003). Samples were prepared by oven drying followed by grinding to pass a 2 mm sieve. Prior to the hydrometer procedure the gravimetric water content of a

subsample (~5 g) of the prepared sample was determined and the result was subtracted from the sample weight in calculations.

2.7 Soil thermal properties. The Decagon KD2 Pro dual-probe, heat pulse sensor was used to determine thermal diffusivity, volumetric heat capacity, thermal conductivity and thermal resistivity of each sample after equilibration at -33 kPa (Bristow *et al.*, 1994). The analysis of these data is outside the scope of this paper.

2.9 Validation Sites. Nine validation sites were selected based on the presence of soil water content sensors to 60 cm as well as varying soil textural classes. Water content was measured at -8, -16, -33, -66, -125, -250, -500, -1,000, and -1,500 kPa for each sample for a total of 45 samples. Equation [2] was then fitted to the points and the measured water retention curves were compared to those estimated by Rosetta. The validation sites were Acme, Burneyville, Byars, Chickasha, El Reno, Eufala, Hobart, Oklahoma City West, and Shawnee.

The accuracy of the Rosetta water retention curves was determined by the root mean squared difference (RMSD), which was found as the deviation from the 1:1 relationship with the measured data as shown in Eq. [5],

$$RMSD = \sqrt{\frac{1}{N}\sum_{i=1}^{N}(\gamma'_i - \gamma_i)^2} \quad \textbf{[5]}$$

and the mean error (ME) to measure over or under estimation by Rosetta when compared to the measured data as Eq. [6]

$$ME = \frac{1}{N}\sum_{i=1}^{N}(\gamma'_i - \gamma_i) \quad \textbf{[6]}$$

where γ' and γ are the estimated and measured values of the variable under consideration and N is the number of measurements. Root mean squared difference was used as opposed to the root meant squared error (RMSE), or deviation from the regression line, because the measured values and those estimated by Rosetta should have a 1:1 relationship.

2.10 Plant available water. PAW at the Mesonet stations is determined by converting volumetric water content into PAW (mm) via Eq. [7]

$$PAW = \sum_{i=1}^{n} \left(\theta_i - \theta_{wpi}\right) dz_i \qquad \textbf{[7]}$$

where θ_i ($cm^3\ cm^{-3}$) is the current volumetric water content of layer *i*, θ_{wpi} ($cm^3\ cm^{-3}$) is the permanent wilting point for layer *i*, dz_i (mm) is the thickness of layer *i*, and *n* is the number of layers. Calculated values of PAW based on the Mesonet sensors were compared to values determined through soil samples taken at each site. Three variations of that comparison were explored. The first method compared PAW by the sensors using the volumetric water content at wilting point, θ_{wpi} ($cm^3\ cm^{-3}$), from the Rosetta van Genuchten parameters with a matric potential of -1500 kPa to PAW by sampling using the θ_{wpi} determined through the pressure plate method. The second method compared PAW by the sensors as in method one with PAW by sampling using the θ_{wpi} from the Rosetta van Genuchten parameters with a matrix potential of -1500 kPa. The third method compared PAW by the sensors using θ_{wpi} determined through the pressure plate method to PAW by sampling using θ_{wpi} determined through the pressure plate method. Each method was analyzed by regression and RMSD to determine which option produced

the best agreement. The point estimates of θ and PAW were then interpolated by kriging to produce continuous surface maps.

2.11 Kriging and Semivariogram. MATLAB BMElib numerical toolbox (Bogaert et al., 2001) was used to compute empirical semivariograms, fit semivariograms models, and krige the θ and PAW data. Ordinary kriging, which assumes no spatial trend, was selected for use as an initial trial and to enable comparison with the results of Lakhankar et al.(2010). Model selection was based on visual inspection of the data.

The semivariance is the variance based on samples separated by a given lag distance (h) and was calculated via Eq. [8], (Pilz, 2008).

$$\gamma(h) = \frac{1}{2N(h)} \sum_{i=1}^{N(h)} (z_i - z_{i+h})^2 \quad \textbf{[8]}$$

where γ(h) = semi-variance for a lag interval group (h), Z_i = measured sample value at point *i*, Z_i+*h* = measured sample value at point *i* + *h*, and N (h) = total number of sample pairs for the lag distance *h* (Lakhankar et al., 2010).

Semivariances over the range of lag distances determined by Eq. [8] were then plotted on a semivariogram. The semivariogram was then used to determine the optimal weights for predicting values at locations that were not measured by Mesonet stations using Eq. [9] (Bolstad, 2008)

$$Q = \sum_{j=1}^{n} w_j * v_j \quad \textbf{[9]}$$

where *Q* is the unknown value, w_j is the weight for each sample *j*, and v_j is the know value at sample point *j* (Bolstad, 2008).

CHAPTER III

RESULTS AND DISCUSSION

3.1 Soil Properties. The resulting Mesonet soil database (Meso-Soil) covers 13 environmental variables with 541 complete replicated sample sets (1,082 individual core sections) that represent combinations of site and depth for 117 Mesonet Stations. The database contains the percent sand, silt, and clay; the bulk density, the volumetric water content at -33, and -1500 kPa; the van Genuchten parameters of residual volumetric water content, θ_r, saturated volumetric water content, θ_s (cm^3 cm^{-3}), alpha, α (kpa^{-1}), and n (unitless); the saturated hydraulic conductivity, K_s (cm day^{-1}), as well as the matching point parameter, K_o (cm day^{-1}), and the empirical parameter, L (unitless). The percent sand, silt, and clay found through the hydrometer method were used to determine the textural class of each sample. Percentages varied from 2 to 88 percent for sand, 0 to 74 percent for silt, and from 4 to 78 percent for clay. Of the 12 major texture classes, all were represented except sand and silt. Fine textures are well represented in the database with 70 percent of samples having greater than 20 percent clay content. The clay and loam classes have the most representation at 85 samples each whereas loamy sand and sandy clay have the least representation at 6 samples each. The textural triangle distribution can be seen in Figure 3.1. After quality control, bulk density measurements of the soil matrix varied from 0.92 to 1.95 g cm^{-3} with an average of 1.50 g cm^{-3}. Water

retention measurements at -33 kPa vary from 0.06 to 0.50 cm cm^{-3} with a mean of 0.28, and at -1500 kPa from 0.01 to 0.35 cm cm^{-3} with a mean of 0.15.

Table 3.1 shows the input variables for Rosetta averaged by textural class including bulk density, percent sand, percent clay, water content at -33 kPa, and water content at -1500 kPa. The percent silt is not included because it was not measured directly, but found through the sum of clay and sand taken from 100 percent. The Meso-Soil database enables the creation of PTFs that are specific to Oklahoma's unique climate. Table 3.2 provides a texture class average hydraulic parameter PTF lookup table for the Meso-Soil database modeled after the Rosetta class average table (Schaap et al., 2001b). The Rosetta class average table has all texture classes represented, however the majority of samples are in the loam and sand texture classes. As determined through textural analysis, the majority of Oklahoma Mesonet station soils are fine textured, making the development of an Oklahoma specific table beneficial. The residual volumetric water content, θ_r, and saturated volumetric water content, θ_s, of the Meso-Soil database tended to be lower than the Rosetta class average values. Alpha, α, and n did not vary significantly between the two datasets. The Meso-Soil database values for saturated hydraulic conductivity, K_s, tended to be lower for finer textures and higher for coarse textures relative to the Rosetta look up table with the largest difference of 197 cm d^{-1} in the loamy sand texture class. The matching point, K_o, followed the same trend as K_s with the largest discrepancy in the loamy sand of 42 cm d^{-1}. The empirical parameter L values are comparable to the Rosetta values with few exceptions, in both datasets L tended to be less than zero.

3.2 Laboratory Water Retention Curve Validation. The Rosetta van Genuchten parameters were able to accurately predict the water retention points measured in the lab. The RMSD was evaluated based on the soil texture families (Baillie, 2001) of coarse loamy with 0-18% clay, fine loamy, with 18-35% clay, fine clayey, with 35-60% clay, and very fine clayey with greater than 60% clay. The relationship between increasing fines, or increase in percent clay, and RMSD was not conclusive with 0.064, 0.050, 0.045, and 0.064 $cm^3\ cm^{-3}$, respectively. However, the water retention curves for the Burneyville site are shown in Figure 3.2. All five depths are sandy loam. The RMSD of the direct fit to Eq. [2] varied from 0.010 to 0.025 ($cm^3\ cm^{-3}$), the RMSD of the Rosetta prediction varied from 0.013 to 0.035 ($cm^3\ cm^{-3}$). The water retention curve established for the Shawnee site, shown in Figure 3.3, represent the finest textures of the 9 validation sites with silt loam at 3-10 cm, silty clay loam at 20-30 cm, and silty clay from 40-80 cm. The greatest deviation from the direct fit data can be seen in the finest textured silty clay from 40-80 cm. The RMSD of the direct fit varied from 0.010 to 0.015 ($cm^3\ cm^{-3}$), the Rosetta prediction RMSD varied from 0.026 in the silty clay loam to 0.068 in the finest textured silty clay. In general, Rosetta tended to better predict the water retention curves for coarse textured soil.

The RMSD and ME for the direct fit of Eq. [2] to the measured water retention data for all of the validation sites and for the water retention curves based on the parameters estimated using Rosetta were determined at each of the 9 pressures as shown in Figure 3.4. The RMSD for all depths and pressures of the direct fit of Eq. [2] to the data was 0.011 $cm^3\ cm^{-3}$ and remained relatively flat with the lowest RMSD of ~0.008 at low and higher pressures. The greatest error of 0.017 occurred at -66 kPa. The RMSD for

all pressures of the Rosetta water retention curves was 0.043 $cm^3\,cm^{-3}$ with a RMSD of ~0.025 at the lowest pressures increasing to a high of 0.060 at -250 kPa and decreasing steadily to 0.037 at -1500 kPa.

The mean error of the direct fit of Eq. [2] to the data was $1.2x10^{-4}$ $cm^3\,cm^{-3}$ with the greatest error of 0.007 $cm^3\,cm^{-3}$ at -33 and -125 kPa. Rosetta tended to underestimate the water content compared to the laboratory measured water retention curve data with a ME of -0.023 $cm^3\,cm^{-3}$. The ME was greatest at -66 and -250 kPa at -0.043 $cm^3\,cm^{-3}$. At matrix potentials near zero, the ME was ~0.01 while at matrix potentials from 500 to 1,500 kPa the mean was -0.03 $cm^3\,cm^{-3}$.

Lab analysis of the Rosetta model was completed by Schaap et al. (2001a) based on the calibration data set by evaluating the root mean square error between measured and estimated water contents. They found that the error decreased with the ANN method versus traditional PTFs as well as decreasing with increased number of input parameters in Rosetta to 0.044 $cm^3\,cm^{-3}$. That value is nearly identical to the 0.043 $cm^3\,cm^{-3}$ RMSD found for our validation data.

3.3 Field θ and PAW Validation. Field validation of the complete Meso-Soil database was verified by comparing the volumetric water content calculated from the Rosetta van Genuchten parameters and the daily average ΔT_{ref} output from the Oklahoma Mesonet 229-L heat dissipation sensors on the day of soil sampling to the volumetric water content determined by oven-drying a sub-sample of the core section (Figure 3.5). The RMSD of the complete dataset was 0.053 $cm^3\,cm^{-3}$, this is the best current estimate for the overall network-wide uncertainty of the Oklahoma Mesonet soil water content

data when using the new Meso-Soil database. The RMSD decreased with depth from 0.061 $cm^3\ cm^{-3}$ at 5cm, to 0.053 at 25, 0.044 at 60, and 0.033 at 75 cm. The slope for the regression was significantly different from one based on the 95% confidence interval, and the intercept is significantly different from zero.

Possible sources of error include variations at the field scale due to the 3 meter spacing between replicate cores, sensor errors present in the ΔT_{ref} values, calculation of matric potential from Eq. [1], error present in the lab measurements, and modeling error present in the Rosetta program. The RMSD between duplicate core sections for the water content at sampling found through oven drying, -33 kPa found through the Tempe cell method, and -1500 found using the pressure cell method were 0.036, 0.040, and 0.038 $cm^3\ cm^{-3}$, respectively. This means that a substantial portion of the 0.053 $cm^3\ cm^{-3}$ overall uncertainty likely arises from small scale spatial variability in soil moisture at the Mesonet sites.

The volumetric water content at sampling estimated from the pre-existing Arya and Paris derived van Genuchten parameters had substantial bias at the dry end as indicated by overestimation of water content (Figure 3.6). The RMSD of the complete dataset was 0.078 $cm^3\ cm^{-3}$ based on sampling of all the Mesonet sites, which is larger than the published values of 0.066 which was based on a smaller subset of sites (Illston et al., 2008). The RMSD decreased with depth from 0.089 $cm^3\ cm^{-3}$ at 5cm, 0.078 at 25, 0.062 at 60, and 0.067 at 75 cm. The slope and intercept for the regression are significantly different from one and zero respectively, based on a 95% confidence interval. The new database led to a 32% improvement in the RMSD of volumetric water content for the Mesonet, therefore previous studies using the Arya and Paris predicted

van Genuchten parameters may be worth reanalyzing with the new Meso-Soil database parameters.

Knowing the soil characteristics lets us estimate the PAW for all sites in the network. Plant available water may be a better variable than volumetric water content for applications such as ecohydrology and agronomy because the characteristics of the soil are taken into account. The PAW option that performed best in comparing sensor data to sampled data was option three which is recommended as the method of use for the Mesonet website. This comparison shown in Figure 3.7 resulted in a RMSD of 19 mm which corresponds approximately to the RMSD value of 0.053 $cm^3 cm^{-3}$ from Figure 3.5 when integrated over the 40 cm profile. The R^2 value was 0.67 with a slope of 0.942 which was not significantly different than one at a 95% confidence interval while the intercept of 10.2 mm was significantly different from 0. Option two resulted in an increase in RMSD to 20 mm and a slight increase in the R^2 value to 0.68. The slope was not significantly different than one at 0.91; however the intercept was significantly different than 12.7 mm. The first option performed the worst with a RMSD of 25 mm and a R^2 of 0.64, the slope and intercept were 0.935 and 19.4, respectively.

3.4 Spatial Variability Analysis.

In Figure 3.8, semivariogram models of the spatial variation in soil water content at the 5 cm depth on a) March 29, 2010 during wet conditions, b) August 07, 2011 during dry conditions, and c) May 15, 2011 during transitional conditions, in Oklahoma are presented. The semivariogram model with the best visual fit for Fig. 3.8a was a combination nugget and Gaussian model. The resulting semivariogram indicates a lack of

spatial structure; the semivariogram is mostly sill with no identifiable range. In contrast, the semivariogram of the dry day, Fig. 3.8b, gives a range of 189 km found when fit with a combined model of nugget and exponential. This is similar to the 175 km range found by Lakhankar et al.(2010). For Fig. 3.8b, the state lacked a strong spatial trend in soil water content due to widespread dry conditions, resulting in an identifiable nugget and sill of $1.4x10^{-3}$ and $3.3x10^{-3}$, respectively. Nugget to sill (N/S) ratios characterize the strength of the spatial structure of the data with the majority of N/S ratios for soil property data ranging from 0.1 to 0.6 for strong to weak spatial structures, respectively (Kravchenko, 2003). The N/S ratio of Figure 3.8b was 0.44, suggesting a weak spatial structure. Whereas, large scale spatial patterns accounted for 66 percent of the mesoscale spatial variance of soil moisture found in the previous study of the Mesonet soil moisture systems (Lakhankar et al., 2010). Figure 3.8c was produced on a precipitation transition day in which approximately half the state had recently experienced precipitation while the rest remained dry. The best visual fit was a combined nugget and Gaussian semivariogram model as in Fig. 3.8a. As expected, this resulted in the greatest spatial variation. The semivariogram was unbounded as a result of the known strong spatial trend in moisture from east to west with no identifiable sill or range. These data demonstrate that soil moisture exhibits spatial structure beyond the 300 km scale.

Figure 3.9a-c are maps created from Figure 3.8a-c semivariograms, respectively. The spacing for the kriging grid was set to 30 km, with the maximum number of neighboring points considered set at 10 and a maximum distance of 100 km. The uncertainty associated with the maps is related to the kriging variance, the square root of which averaged, 0.076, 0.052, and 0.085 $cm^3\ cm^{-3}$ for Figs. 3.9a-c, respectively. Clearly,

a large, dynamic range of soil water content conditions exist with the spatial structure changing over time. The Meso-Soil database and Oklahoma Mesonet sensor data present many opportunities for research on the spatial and temporal variability of soil water content at the state scale. These maps may be particularly valuable for evaluating large-scale remotely-sensed or modeled soil moisture.

Plant available water may be a better variable than soil water content for mapping because PAW integrates multiple sensor depths, accounts for differences in soil type, and is more closely related to plant water stress. One application of the Meso-Soil database is the creation of PAW semivariograms and maps. Figure 3.10a-c and 3.11a-c show semivariograms and maps of PAW in the 0-40 cm soil layer for the a) wet, b) dry, and c) transition days used in Fig. 3.8. The semivariogram models with the best visual fit for PAW were consistent with those for soil water content. The square root of the kriging variance averaged, 19.7, 8.5, and 23.7 mm for Figs. 3.11a-c, respectively. The assumption of no spatial trend required in ordinary kriging was violated in Figures 3.10a and c as indicated by the unbounded structure of the semivariograms. More research needs to be done to determine how to best detrend these data. These are the first known semivariograms and maps for PAW. Nonetheless, Fig. 3.10 provides some evidence that PAW can exhibit stronger spatial structure than soil water content. For example, the maximum semivariance in Fig. 3.10c is four times the minimum semivariance, whereas in Fig. 3.8c the maximum semivariance is only twice the minimum semivariance. The new soil database, combined with the Mesonet sensors, create rich opportunities to explore the spatial structure of this key variable.

The development of the Meso-Soil soil property database combined with the archived data of the Oklahoma Mesonet provides opportunities to study existing theories regarding preferential states in soil water content (D'Odorico et al., 2000) and soil, plant, atmosphere coupling (Chen et al., 2011). Studies that examine these phenomena often look at frequency distributions of soil water content (D'Odorico et al., 2000). Figure 3.12 shows the frequency distributions of PAW in the 0-40 cm layer at the Oklahoma Mesonet stations Goodwell, Norman, and Idabel which span a northwest to southeast transect across the state. All stations are still actively recording data; the Goodwell station began recording soil moisture data in August of 1997, Norman in September of 2002, and Idabel in June of 1999. The frequency distribution of the Goodwell site indicates primarily dry conditions with plant available water below 25 mm occurring 50 percent of the time. The Idabel site tended to be wet with PAW of 75 mm or greater over 50 percent of the time. These results are as expected with Oklahoma's strong precipitation gradient which increases from northwest to southeast. However, the frequency distribution at the Norman site was strongly bimodal with PAW of 25 mm or less over 30 percent of the time and PAW of 75 or greater approximately 40 percent of the period of study. These findings are consistent with the hypothesis that soil water deficits have a positive feedback effect on drought by reducing the probability of precipitation. This in turn results in two preferential states of wet or dry, with a low frequency of occurrence of intermediate conditions in soil water content (D'Odorico et al., 2000). Oklahoma's uniquely varying climate provides an opportunity to further study the causes of these preferential states and their effects on prolonged drought.

Oklahoma Mesonet has been archiving soil water content data at many locations since 1996. Because of the length of the data record, these stations can begin to be used in climatology studies across the large climate gradient of Oklahoma. For example, time series of soil water content allow visualization of anomalous events such as the droughts of 2006 and 2011. In Fig. 3.13, a severe drought is reflected in an extended period of unusually low water content at the 60 cm depth in a time series analysis of the Stillwater Mesonet station from January, 2011 to December, 2012. As expected, the 5 cm VWC has high frequency variations at shorter time scales, while deeper depths respond more slowly. These kinds of data are especially useful in evaluating model predictions of soil moisture variation with depth and time at individual locations.

CHAPTER IV

CONCLUSIONS

The soil property database will be available for download from the Oklahoma Mesonet website; www.mesonet.org.

In order to simplify the conversion of the sensor ΔT_{ref} data to volumetric water content and plant available water, two Matlab functions were created. MesothetaS facilitates spatial investigation using a single day of data. It provides three outputs, the volumetric soil water content for the 5, 25, and 60 cm sensors for each station, the plant available water for the 0-10, 0-40, and 0-80 cm layers at of each station, and a map of PAW produced by ordinary kriging. Inputs required to run the function include the ΔT_{ref} data for each station for the selected day and the soil property database file. MesothetaT is a function which interprets a time series of data for a single site. The outputs include soil water content for the 5, 25, and 60 cm depths, plant available water for the 0-10, 0-40, and 0-80 cm layers, and a time series plot of PAW for the available sensor depths. The inputs required include the Mesonet ΔT_{ref} data for a single site during the time period of interest and the soil property database file. Both Matlab functions will be available for download on the Oklahoma State University Soil Physics Website, http://soilphysics.okstate.edu/.

Through the development of the Oklahoma Mesonet Soil Property database the accuracy of soil water content measurement has been improved by 32% for the Mesonet system. The RMSD between the values found through direct measurement and those found using the 229-L sensor with the new soil properties was 0.053 cm^3 cm^{-3} while the corresponding value with the pre-existing soil database was 0.078 cm^3 cm^{-3}. The measurement of the additional soil properties of water retention at -33 kPa and -1500 kPa along with the neural network model Rosetta enabled this improvement in the accuracy of soil water content measurement based on Mesonet ΔT_{ref} data. Another major benefit of having such a detailed and extensive database of the Mesonet station soils is future adaptability. As more effective pedo-transfer functions are developed, the existing database can be utilized as input parameters allowing for further increases in accuracy of soil water content measurement.

Oklahoma Mesonet products that utilize the new database are currently in use and under development. One product resulting from this work that is currently available on the website is the daily plant available water maps that provide the 4, 16, and 32 inch depth plant available water in inches (http://www.mesonet.org/index.php/weather/category/soil_moisture_temperature). These PAW maps allow for quick and easy interpretation versus the previous mapping variable, fractional water index, a unitless measure of the ratio of the current conditions to the sensor extremes. Currently, the OK-FIRE division of the Mesonet is working to incorporate plant available water data into models that predict fire danger. The plant available water data will be used in fuel moisture models that predict the amount of moisture present in vegetation.

Continued research on the spatial structure of plant available water is needed. The results of the semivariogram analysis suggested a stronger spatial pattern in PAW than in soil water content. The stronger spatial pattern may result from the fact that PAW accounts for spatial variations in soil water retention at -1500 kPa. However, of the three days analyzed only the dry day had a meaningful nugget to sill ratio, allowing a clear estimate of the strength of the spatial structure. The unbounded shape of the wet and transitional moisture days are evidence of the large-scale spatial trends present in the data. Determining a method of successfully detrending the data, or research into more flexible methods of spatial interpolation, are necessary.

Table 3.1 Textural class average, bulk density, particle size percent, and water content for the soils of the Oklahoma Mesonet stations. Number of samples in each textural class (N), bulk density (ρb), percent sand, percent clay, water content at -33 kPa (θ_{-33}), and water content at -1500 kPa (θ_{-1500}). Percent silt was determined as the difference between 100 percent and the sum of clay and sand and is therefore not shown.

Textural Class	N	ρb		sand		clay		θ_{-33}		θ_{-1500}	
		(g cm^{-3})		(%)		(%)		(cm^3 cm^{-3})		(cm^3 cm^{-3})	
Clay	85	1.52	(0.16)	17.4	(9.4)	52.8	(8.6)	0.38	(0.06)	0.25	(0.05)
C Loam	83	1.51	(0.15)	30.6	(6.3)	32.9	(3.7)	0.28	(0.05)	0.15	(0.04)
Loam	85	1.46	(0.15)	41.1	(6.0)	20.7	(4.2)	0.23	(0.05)	0.09	(0.03)
L Sand	6	1.49	(0.21)	81.7	(3.8)	6.9	(2.9)	0.09	(0.02)	0.02	(0.01)
Sand	N/A	-	-	-	-	-	-	-	-	-	-
S Clay	6	1.67	(0.15)	53.7	(4.6)	40.5	(5.8)	0.34	(0.03)	0.21	(0.03)
S C L	37	1.57	(0.19)	55.7	(7.4)	25.8	(4.1)	0.22	(0.05)	0.12	(0.04)
S Loam	58	1.51	(0.21)	66.5	(9.5)	12.8	(3.9)	0.16	(0.05)	0.06	(0.02)
Silt	N/A	-	-	-	-	-	-	-	-	-	-
Si C L	56	1.45	(0.20)	13.2	(4.7)	33.9	(3.7)	0.28	(0.05)	0.10	(0.03)
Si Clay	55	1.58	(0.13)	9.9	(4.3)	45.3	(3.6)	0.38	(0.05)	0.25	(0.05)
Si Loam	70	1.48	(0.18)	21.1	(7.6)	18.7	(4.6)	0.31	(0.05)	0.17	(0.05)

Table 3.2 Textural class average hydraulic parameters for the soils of the Oklahoma Mesonet stations. Number of samples in each textural class (N), residual water content (θ_r), saturated water content (θ_s), fitting parameters alpha (α) and n, saturated hydraulic conductivity (K_s), fitted matching point at saturation (K_o), empirical parameter (L).

Textural Class	N	θ_r		θ_s		α		n		K_s		K_o		L	
		($cm^3\ cm^{-3}$)		($cm^3\ cm^{-3}$)		($1\ kPa^{-1}$)		(unitless)		($cm\ d^{-1}$)		($cm\ d^{-1}$)		(unitless)	
Clay	85	0.07	(0.01)	0.45	(0.04)	0.13	(0.10)	1.26	(0.10)	11.3	(15.2)	3.5	(3.2)	-1.2	(1.5)
C Loam	83	0.06	(0.01)	0.40	(0.03)	0.16	(0.12)	1.36	(0.11)	13.7	(11.5)	7.1	(9.1)	-0.7	(0.7)
Loam	85	0.04	(0.01)	0.38	(0.03)	0.16	(0.10)	1.43	(0.10)	22.7	(14.7)	8.7	(8.1)	-0.4	(0.6)
L Sand	6	0.02	(0.01)	0.38	(0.05)	0.58	(0.15)	1.55	(0.15)	302.5	(201)	67.0	(48.2)	-1.1	(0.1)
Sand	N/A	-	-	-	-	-	-	-	-	-	-	-	-	-	-
S Clay	6	0.06	(0.01)	0.39	(0.04)	0.11	(0.11)	1.28	(0.06)	16.8	(33.0)	3.9	(4.4)	-0.6	(1.1)
S C L	37	0.05	(0.01)	0.38	(0.04)	0.29	(0.16)	1.35	(0.06)	60.0	(73.2)	16.9	(19.1)	-1.2	(0.6)
S Loam	58	0.03	(0.01)	0.37	(0.05)	0.35	(0.18)	1.41	(0.08)	101.5	(97.6)	26.6	(22.5)	-0.9	(0.6)
Silt	N/A	-	-	-	-	-	-	-	-	-	-	-	-	-	-
Si C L	56	0.07	(0.03)	0.42	(0.03)	0.16	(0.12)	1.36	(0.13)	10.3	(7.2)	5.4	(7.6)	-1.1	(1.8)
Si Clay	55	0.08	(0.01)	0.43	(0.03)	0.16	(0.11)	1.25	(0.12)	3.7	(4.4)	3.5	(2.1)	-2.2	(2.3)
Si Loam	70	0.04	(0.02)	0.39	(0.04)	0.09	(0.10)	1.58	(0.25)	22.5	(27.1)	4.6	(6.2)	0.1	(0.6)

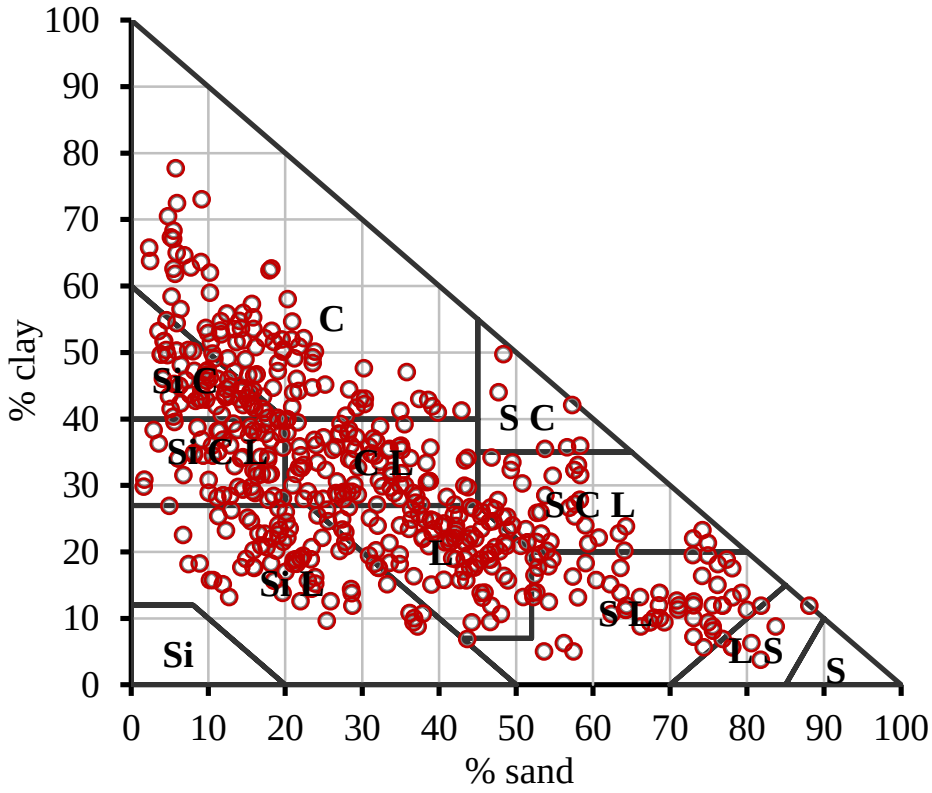

Figure 3.1 Particle size distribution for the soils of the Oklahoma Mesonet stations at the sampled depths (○).

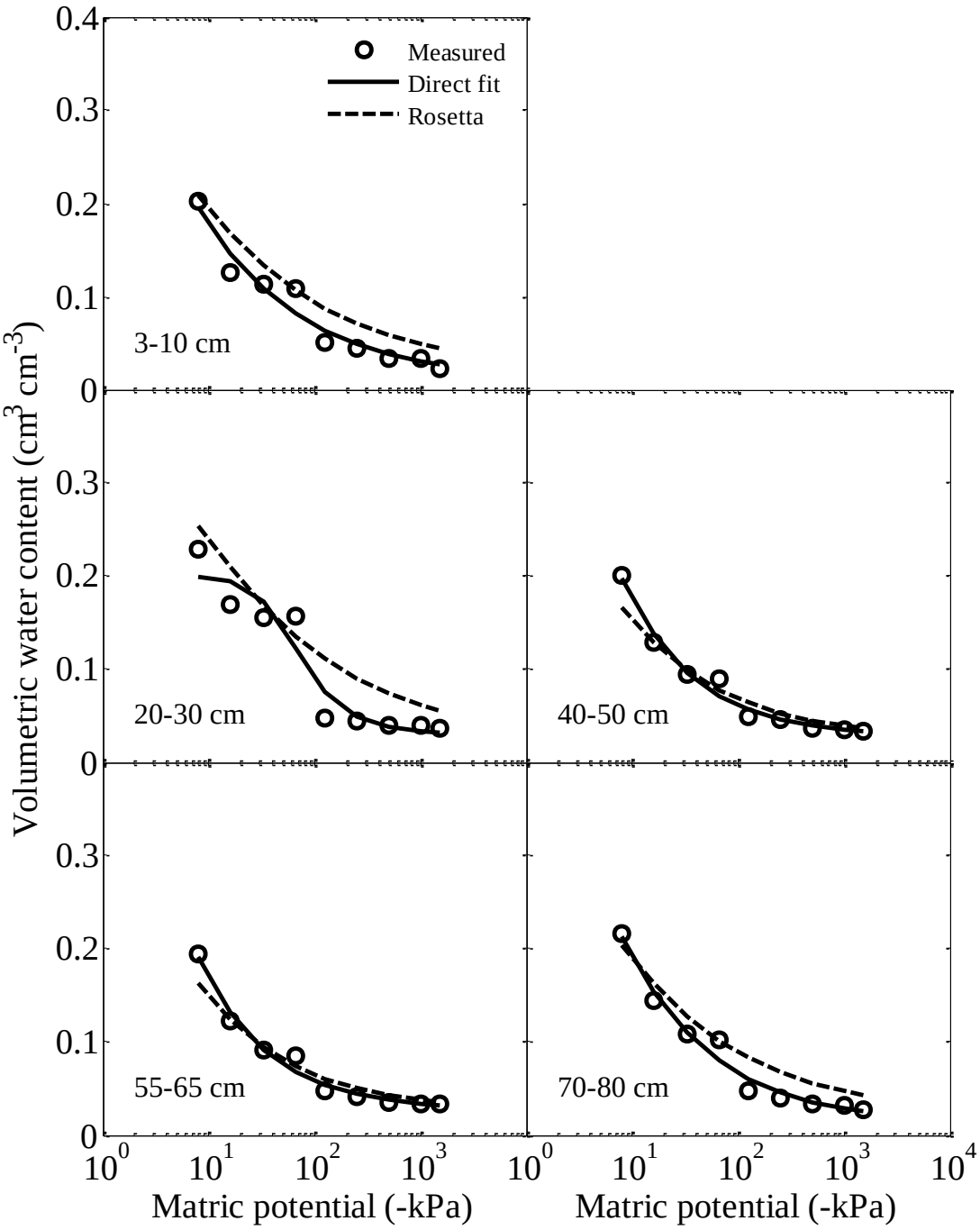

Figure 3.2 Measured water retention curve (○), direct fit of Eq. [3] to the measured data (-), and water retention curve based on the parameters estimated using Rosetta (- -), for the Burneyville Mesonet station by sampling depth. All depths are sandy loam.

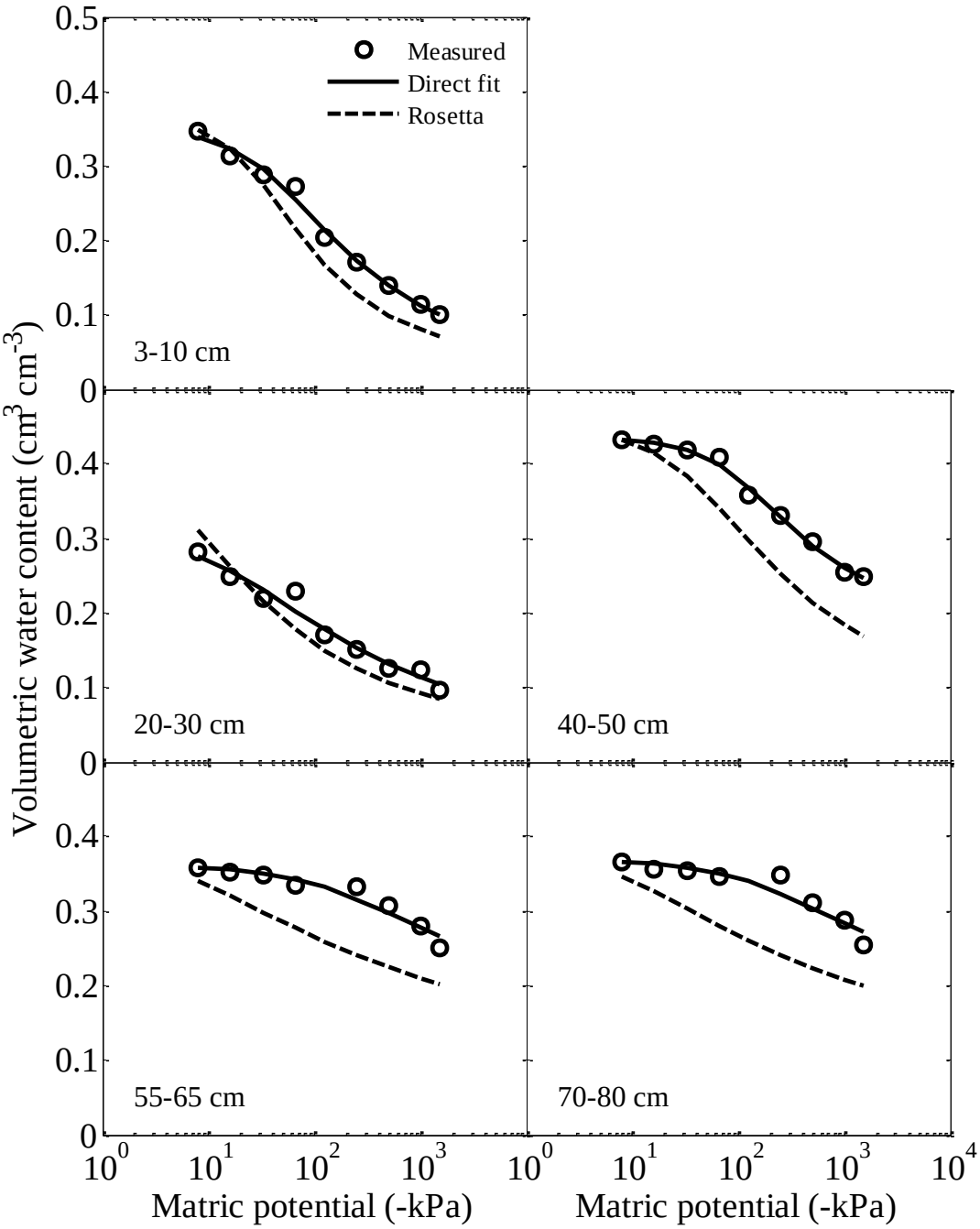

Figure 3.3 Measured water retention curve (○), direct fit of Eq. [3] to the measured data (-), and water retention curve based on the parameters estimated using Rosetta (- -), for the Shawnee Mesonet station by sampling depth. All depths are fine textures with silt loam at 3-10 cm, silty clay loam at 20-30 cm, and silty clay from 40-80 cm.

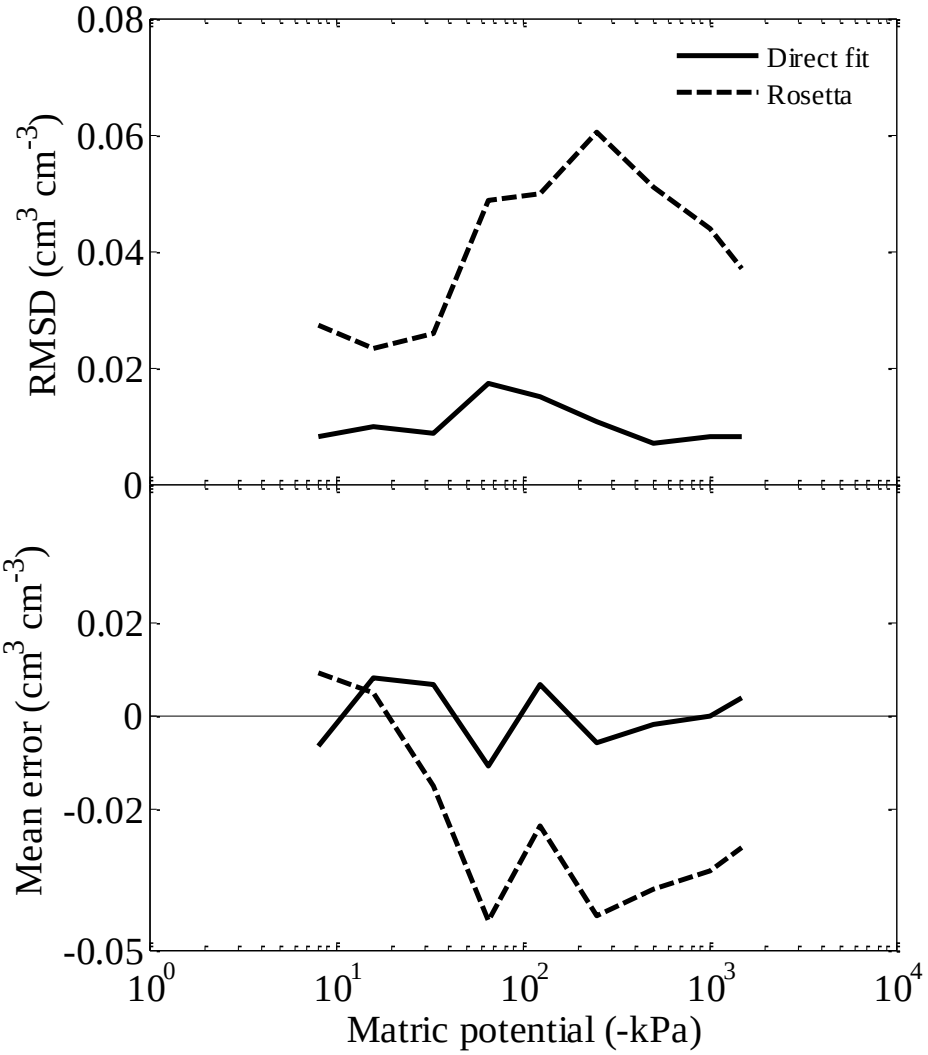

Figure 3.4 Root mean square error (RMSD) and mean error for direct fit of Eq. [3] to the measured water retention data for the validation sites (-) and for the water retention curves based on the parameters estimated using Rosetta (- -).

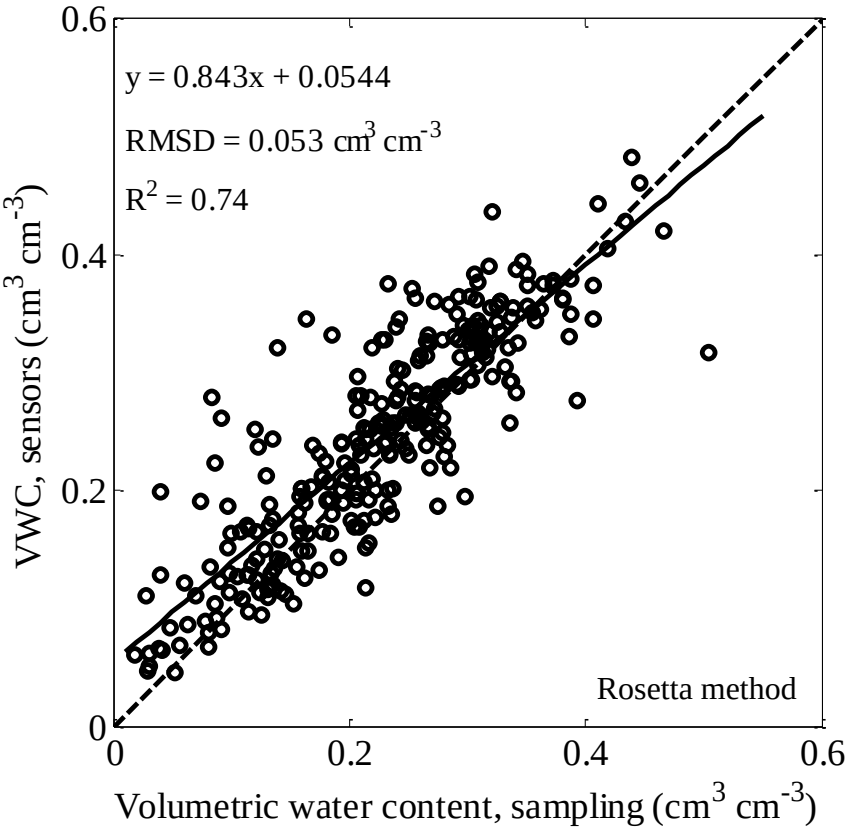

Figure 3.5 Volumetric water content calculated from the daily average ΔT_{ref} output from the Oklahoma Mesonet 229-L heat dissipation sensors on the day of soil sampling (VWC, sensors) versus volumetric water content determined by oven-drying a sub-sample of the core section. The ΔT_{ref} values were converted to ψ_m by Eq. [1] and then to VWC by Eq. [3] using the parameters in the new database. Where (○) is the VWC data, (-) is the regression line, and (- -) is the 1:1 line.

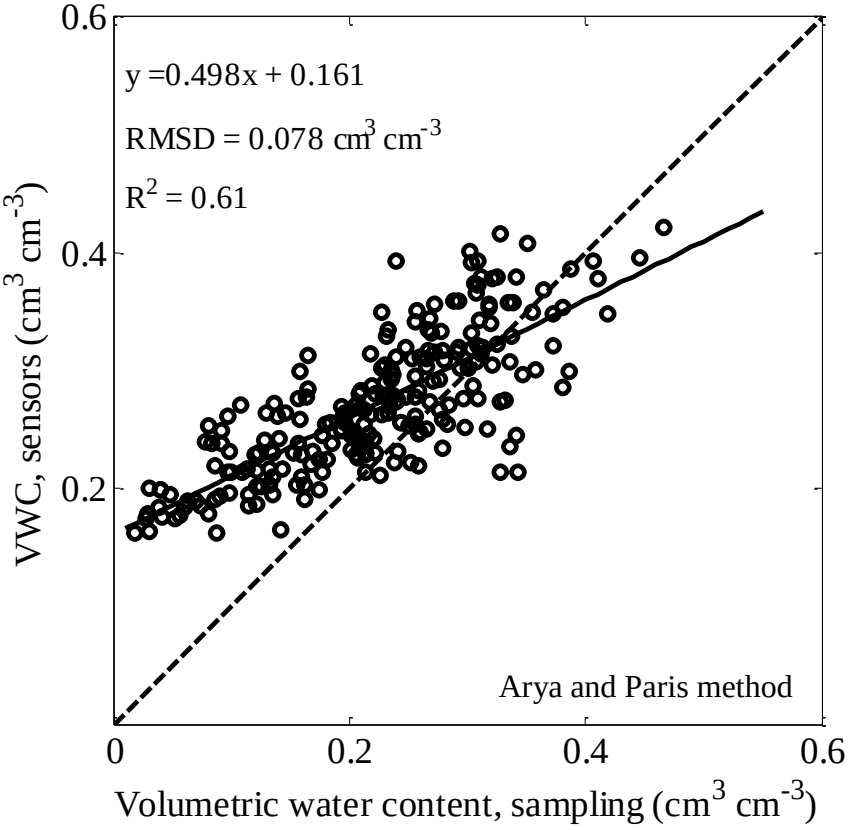

Figure 3.6 Volumetric water content calculated from the daily average ΔT_{ref} output from the Oklahoma Mesonet 229-L heat dissipation sensors on the day of soil sampling (VWC, sensors) versus volumetric water content determined by oven-drying a sub-sample of the core section. The ΔT_{ref} values were converted to ψ_m by Eq. [1] and then to VWC by Eq. [3] using the existing parameters found by the Arya and Paris method. Where (○) is the VWC data, (-) is the regression line, and (- -) is the 1:1 line.

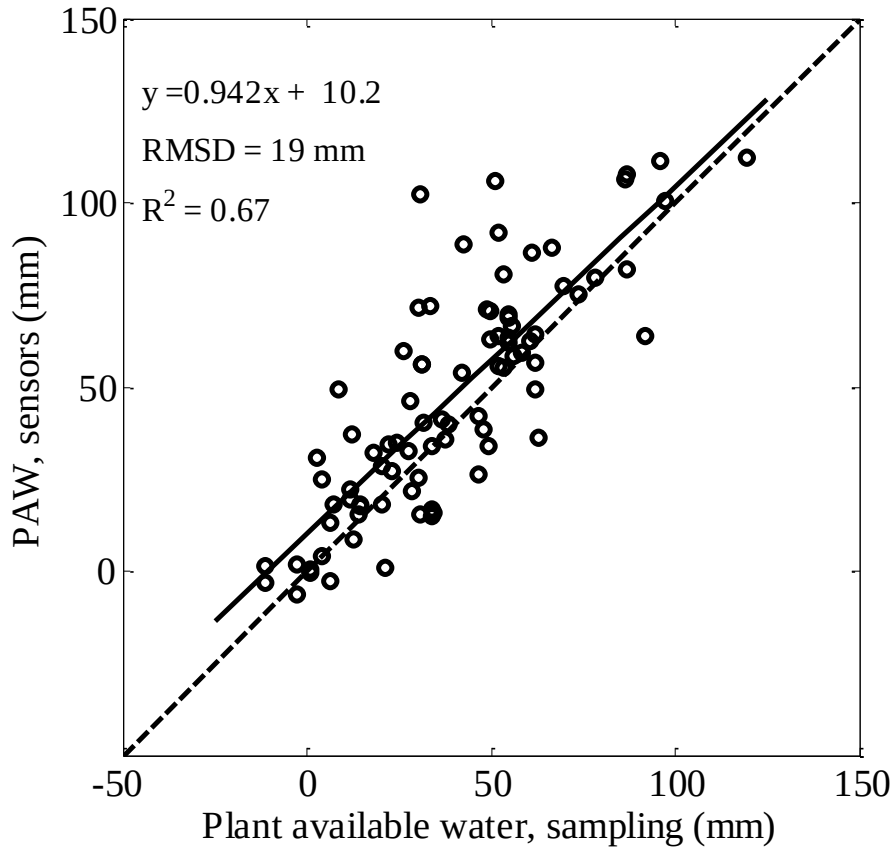

Figure 3.7 Plant available water for 0-40 cm calculated from Eq. [6] where θ_i is the current volumetric water content (VWC) found through the daily average ΔT_{ref} output from the Oklahoma Mesonet 229-L heat dissipation sensors on the day of soil sampling converted to ψ_m by Eq. [1] and then to VWC by Eq. [3] using the parameters in the new database minus the θ_{wpi} as the VWC found via the pressure plate method (PAW, sensors) versus plant available water determined by oven-drying a sub-sample of the core section as θ_i minus θ_{wpi} found via pressure plate. Where (○) is the PAW data, (-) is the regression line, and (- -) is the 1:1 line.

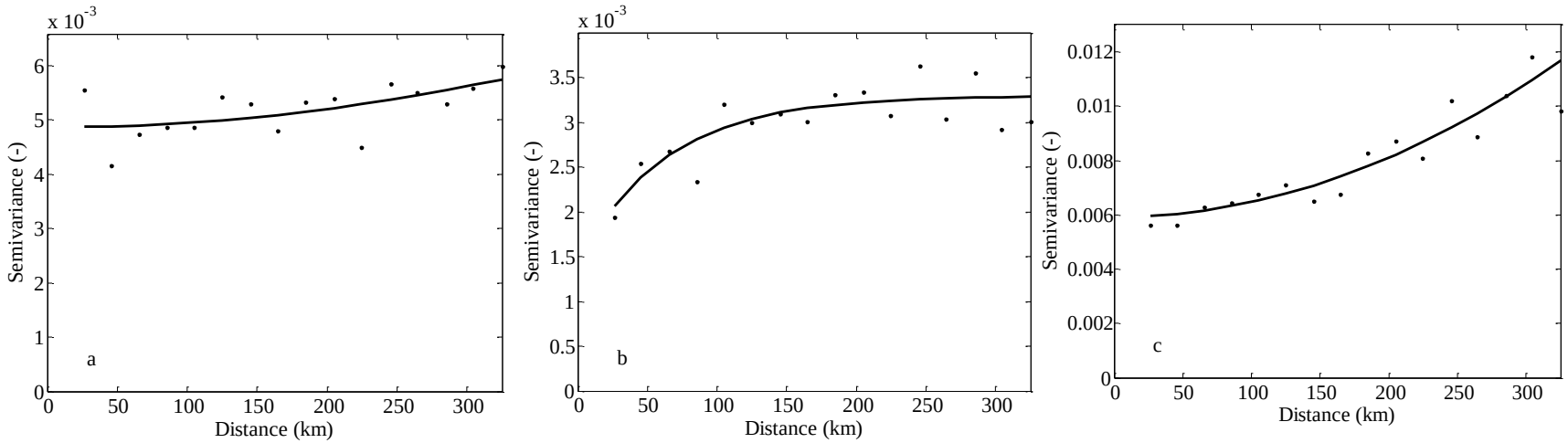

Figure 3.8 Soil water content semivariograms of the Oklahoma Mesonet stations during (a) wet, (b) dry, and (c) transitional moisture conditions on 3/29/2010, 8/07/2011, and 5/15/2011 respectively, where (●) are the empirical semi-variances and (-) are the fitted models. Semivariograms (a) and (c) are combination nugget, Gaussian models, whereas (b) is a nugget, exponential model.

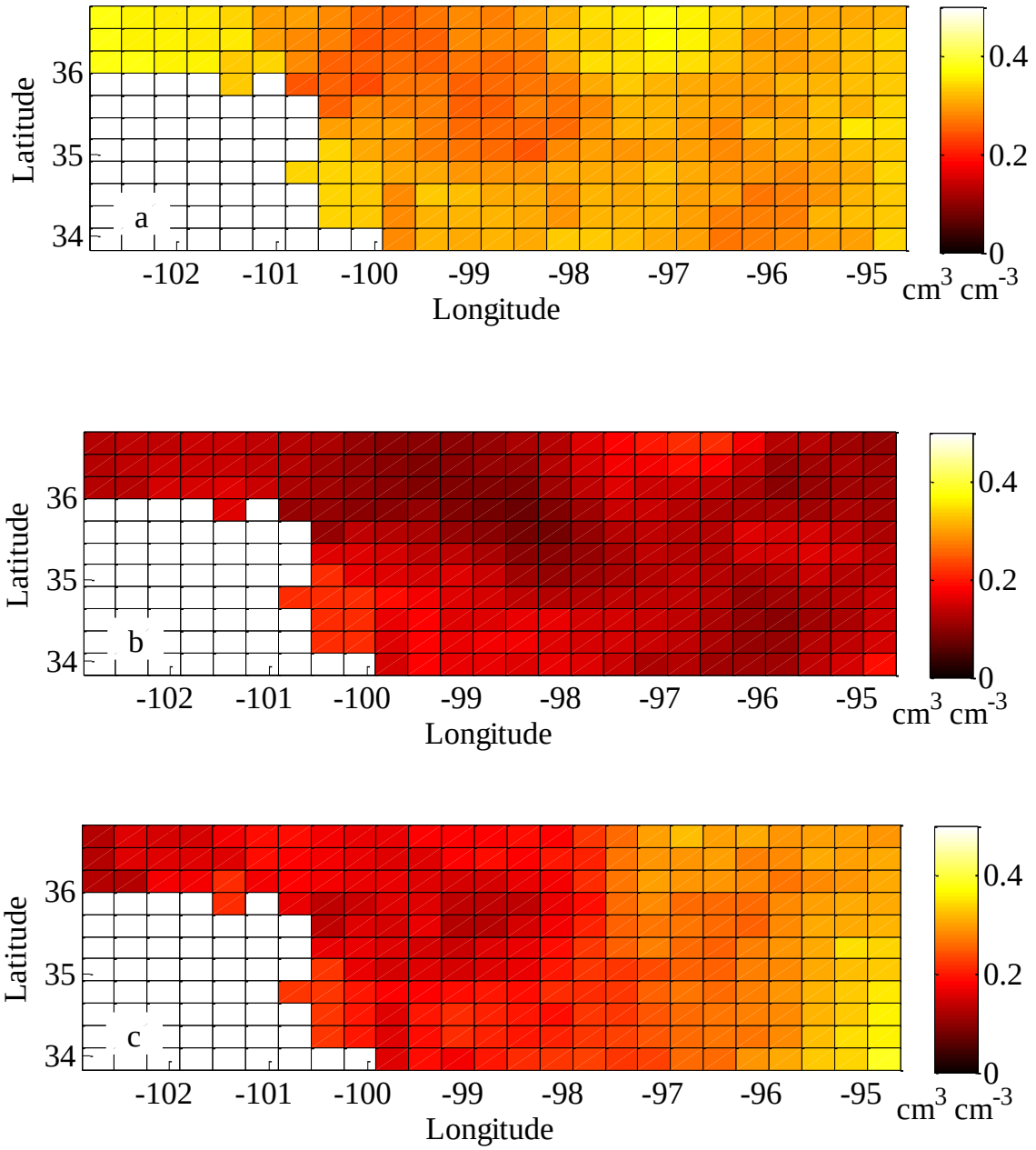

Figure 3.9 Kriged maps of soil water content for Oklahoma Mesonet stations generated using Figure 3.8 semivariograms during (a) wet, (b) dry, and (c) transitional moisture conditions on 3/29/2010, 8/07/2011, and 5/15/2011, respectively.

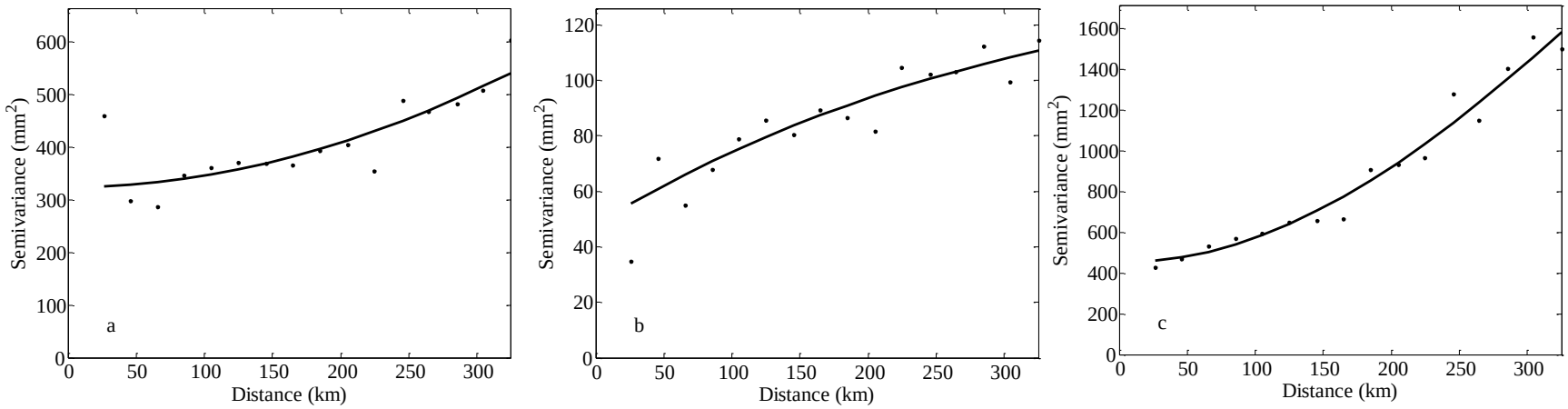

Figure 3.10 Plant available water semivariograms of the Oklahoma Mesonet stations during (a) wet, (b) dry, and (c) transitional moisture conditions on 3/29/2010, 8/07/2011, and 5/15/2011, respectively, where (●) are the empirical semi-variances and (-) are the fitted models. Semivariograms (a) and (c) are nugget, Gaussian models, whereas (b) is a nugget, exponential model.

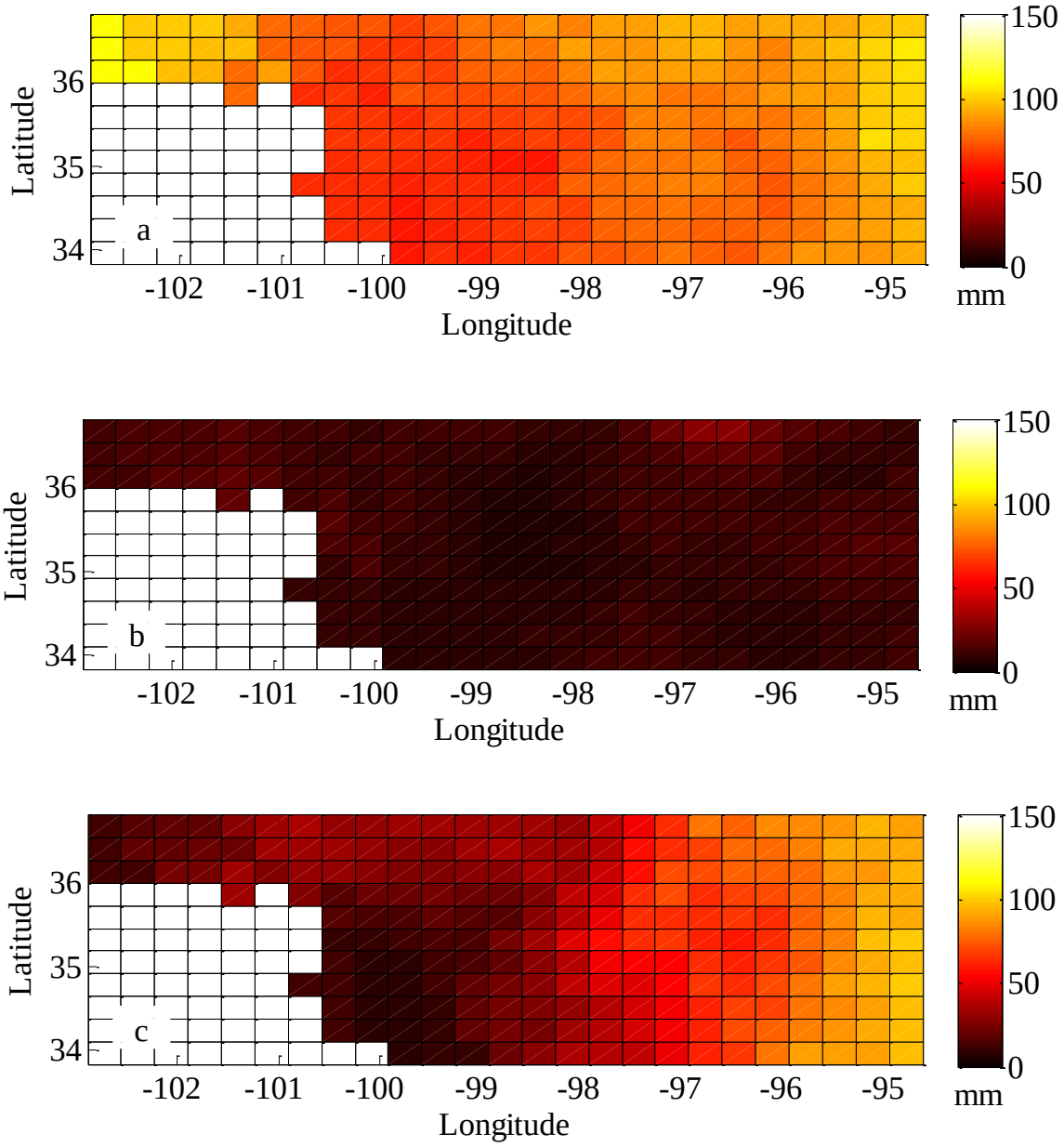

Figure 3.11 Kriged maps of plant available water for Oklahoma Mesonet stations generated using Figure 3.10 semivariograms during (a) wet, (b) dry, and (c) transitional moisture conditions on 3/29/2010, 8/07/2011, and 5/15/2011, respectively.

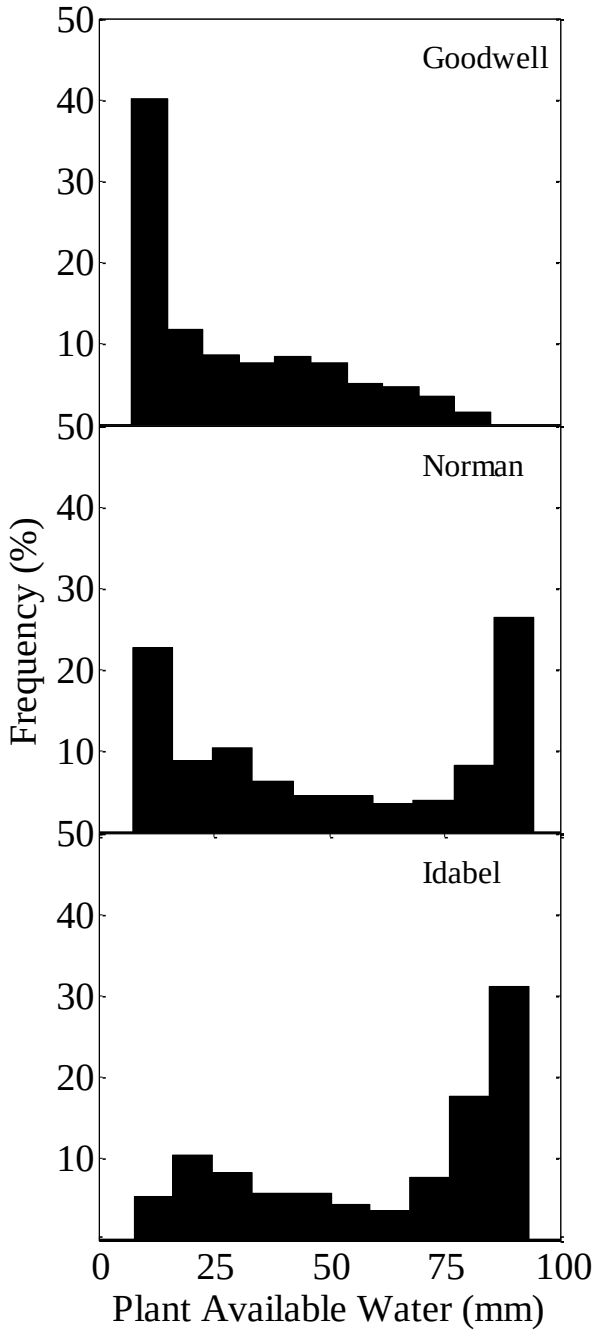

Figure 3.12 Frequency distributions of daily averaged plant available water in a northwest to southeast transect of low to high precipitation. Goodwell is in the Oklahoma panhandle, Norman is near the center of the state, and Idabel is in the far southeast.

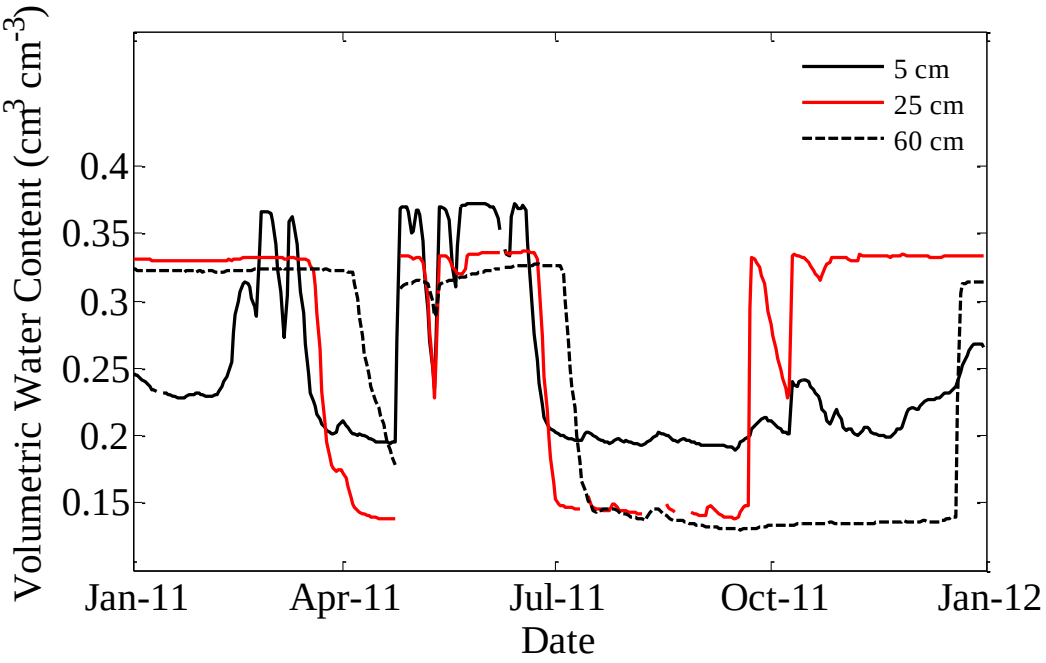

Figure 3.13 Partial time series of volumetric water content for the 5 cm (-), 25 cm (-) and 60 cm (- -) sensors of the Stillwater Oklahoma Mesonet station from January, 20011 to December, 2011. Data is available for the Stillwater site from 1996 to present.

REFERENCES

Ahuja, L.R., J.W. Naney, and R.D. Williams. 1985. Estimating soil water characteristics from simpler properties or limited data. Soil Science Society of America Journal 49:1100-1105.

Arndt, D. 1997. Oklahoma's Climate: An Overview. Available at http://climate.mesonet.org/county_climate/Products/oklahoma_climate_overview.pdf (accessed 07/29/2012).

Arya, L.M., and J.F. Paris. 1981. A PHYSICOEMPIRICAL MODEL TO PREDICT THE SOIL-MOISTURE CHARACTERISTIC FROM PARTICLE-SIZE DISTRIBUTION AND BULK-DENSITY DATA. (in English) Soil Science Society of America Journal 45:1023-1030.

Baarstad, L.L., R.W. Rickman, D. Wilkins, and S. Morita. 1992. A hydraulic soil sampler providing minimum field plot disruption. (in English) Agronomy Journal 85:178-181.

Baillie, I.C. 2001. Soil Survey Staff 1999, Soil Taxonomy. Soil Use and Management 17:57-60.

Bogaert, P., M. Serre, and G. Christakos. 2001. BMElib The University of North Carolina, Chapel Hill, NC.

Bolstad, P. 2008. GIS Fundamentals. 3rd ed. Eider Press, White Bear Lake, MN.

Brady, N.C., and R.R. Weil. 1999. The nature and properties of soils Prentice Hall.

Bristow, K.L., G.J. Kluitenberg, and R. Horton. 1994. Measurement of soil thermal properties with a dual-probe heat-pulse technique. Soil Science Society of America Journal 58:1288-1294.

Brocca, L., T. Tullo, F. Melone, T. Moramarco, and R. Morbidelli. 2012. Catchment scale soil moisture spatial–temporal variability. Journal of Hydrology 422–423:63-75.

Brock, F.V., K.C. Crawford, R.L. Elliott, G.W. Cuperus, S.J. Stadler, H.L. Johnson, and M.D. Eilts. 1995. The Oklahoma Mesonet: A Technical Overview. Journal of Atmospheric and Oceanic Technology 12:5-19.

Chen, F., W.T. Crow, P.J. Starks, and D.N. Moriasi. 2011. Improving hydrologic predictions of a catchment model via assimilation of surface soil moisture. Advances in Water Resources 34:526-536.

Choi, M., J.M. Jacobs, and M.H. Cosh. 2007. Scaled spatial variability of soil moisture fields. Geophys Res Lett 34:L01401.

D'Odorico, P., L. Ridolfi, A. Porporato, and I. Rodriguez-Iturbe. 2000. Preferential states of seasonal soil moisture: The impact of climate fluctuations. Water Resour Res 36:2209-2219.

Dane, J.H., and J.W. Hopmans. 2002. 3.3 Water Retention and Storage: 3.3.2 Laboratory, p. 671-690, *In* J. H. Dane and G. C. Topp, (eds.) Methods of Soil Analysis Part 4 - Physical Methods. ed. Ser. 5. Soil Science Society of America, Inc., Madison, WI.

DeLiberty, T., and D. Legates. 2008. Spatial Variability and Persistence of Soil Moisture in Oklahoma. Physical Geography 29:121-139.

DeLiberty, T.L., and D.R. Legates. 2003. Interannual and seasonal variability of modelled soil

moisture in Oklahoma, pp. 1057-1086, Vol. 23. John Wiley & Sons, Ltd.
Flint, A.L., G.S. Campbell, K.M. Ellett, and C. Calissendorff. 2002. Calibration and temperature correction of heat dissipation matric potential sensors. Soil Science Society of America Journal 66:1439-1445.
Gavlak, R.G., D.A. Horneck, R.O. Miller, J. Kotuby-Amacher, W.R.D. Center, F.W. Fertilizer, and A. Association. 2003. Plant, Soil, and Water Reference Methods for the Western Region Western Rural Development Center.
Godfrey, C.M., and D.J. Stensrud. 2008. Soil Temperature and Moisture Errors in Operational Eta Model Analyses. Journal of Hydrometeorology 9:367-387.
Grossman, R.B., and T.G. Reinsch. 2002. 2.1 Bulk Density and Linear Extensibility: 2.1.1.4 Dealing with Rock Fragments, 2.1.2 Core Method, p. 205-210, *In* J. H. Dane and G. C. Topp, (eds.) Methods of Soil Analysis Part 4 - Physical Methods. ed. Ser. 5. Soil Science Society of America, Inc., Madison, WI.
Hillel, D. 2004. Introduction to environmental soil physics Elsevier Academic Press, Amsterdam ; Boston.
Holmes, T.R.H., T.J. Jackson, R.H. Reichle, and J.B. Basara. 2012. An assessment of surface soil temperature products from numerical weather prediction models using ground-based measurements. Water Resources Research 48:W02531.
Illston, B.G., J.B. Basara, and K.C. Crawford. 2004. Seasonal to interannual variations of soil moisture measured in Oklahoma. International Journal of Climatology 24:1883-1896.
Illston, B.G., J.B. Basara, D.K. Fisher, R. Elliot, C.A. Fiebrich, K.C. Crawford, K. Humes, and E. Hunt. 2008. Mesoscale monitoring of soil moisture across a statewide network. Journal of Atmospheric and Oceanic Technology 25:167-182.
Johnson, K.S. 2008. Geologic History of Oklahoma. Available at http://www.ogs.ou.edu/pubsscanned/EP9_2-8geol.pdf. Oklahoma Geological Survey, Norman, OK.
Kravchenko, A.N. 2003. Influence Of Spatial Structure On Accuracy Of Interpolation Methods. Soil Sci Soc Am J 67:1564-1571.
Lakhankar, T., A.S. Jones, C.L. Combs, M. Sengupta, T.H. Vonder Haar, and R. Khanbilvardi. 2010. Analysis of large scale spatial variability of soil moisture using a geostatistical method. Sensors 10:913-932.
McPherson, R.A., C.A. Fiebrich, K.C. Crawford, J.R. Kilby, D.L. Grimsley, J.E. Martinez, J.B. Basara, B.G. Illston, D.A. Morris, K.A. Kloesel, A.D. Melvin, H. Shrivastava, J.M. Wolfinbarger, J.P. Bostic, D.B. Demko, R.L. Elliott, S.J. Stadler, J.D. Carlson, and A.J. Sutherland. 2007. Statewide Monitoring of the Mesoscale Environment: A Technical Update on the Oklahoma Mesonet. Journal of Atmospheric and Oceanic Technology 24:301-321.
Mohanty, B.P., P.J. Shouse, D.A. Miller, and M.T. van Genuchten. 2002. Soil property database: Southern Great Plains 1997 Hydrology Experiment. Water Resources Research 38.
Pilz, J. 2008. Interfacing Geostatistics and GIS. Spring Science and Buisness Media.
Schaap, M.G., F.J. Leij, and M.T. van Genuchten. 1998. Neural network analysis for hierarchical prediction of soil hydraulic properties. Soil Science Society of America Journal 62:847-855.
Schaap, M.G., F.J. Leij, and M.T. van Genuchten. 2001a. ROSETTA: a computer program for estimating soil hydraulic parameters with hierarchical pedotransfer functions. Journal of Hydrology 251:163-176.

Schaap, M.G., F.J. Leij, and M.T. van Genuchten. 2001b. ROSETTA Class Average Hydraulic Parameters. Available at http://www.ars.usda.gov/Services/docs.htm?docid=8955. Agricultural Research Service.

Schaap, M.G., A. Nemes, and M.T. van Genuchten. 2004. Comparison of Models for Indirect Estimation of Water Retention and Available Water in Surface Soils. Vadose Zone J 3:1455-1463.

Swenson, S., J. Famiglietti, J. Basara, and J. Wahr. 2008. Estimating profile soil moisture and groundwater variations using GRACE and Oklahoma Mesonet soil moisture data. Water Resources Research 44:W01413.

Topp, G.C., and P.A.T. Ferre'. 2002. 3.1 Water Content: 3.1.2.1 Thermogravimetric Method Using Convection Oven-Drying, p. 419, *In* J. H. Dane and G. C. Topp, (eds.) Methods of Soil Analysis Part 4 - Physical Methods ed. Ser. 5. Soil Science Society of America, Inc. , Madison, WI.

Vangenuchten, M.T. 1980. A CLOSED-FORM EQUATION FOR PREDICTING THE HYDRAULIC CONDUCTIVITY OF UNSATURATED SOILS. Soil Science Society of America Journal 44:892-898.

Vereecken, H., M. Weynants, M. Javaux, Y. Pachepsky, M.G. Schaap, and M.T. van Genuchten. 2010. Using Pedotransfer Functions to Estimate the van Genuchten-Mualem Soil Hydraulic Properties: A Review. (in English) Vadose Zone J 9:795-820.

Vinnikov, K.Y., A. Robock, N.A. Speranskaya, and C.A. Schlosser. 1996. Scales of temporal and spatial variability of midlatitude soil moisture. Journal of Geophysical Research 101:7163-7174.

Ward, A.D., and A.D.W.S.W. Trimble. 2004. Environmental Hydrology, Second Edition Lewis Publ.

APPENDIX I

The following seven figure are the measured water retention curve (○), direct fit of Eq. [3] to the measured data (-), and water retention curve based on the parameters estimated using Rosetta (- -), for the validation Mesonet stations by sampling depth in the following order Acme, Byars, Chickasha, El Reno, Eufala, Hobart, and Oklahoma City West.

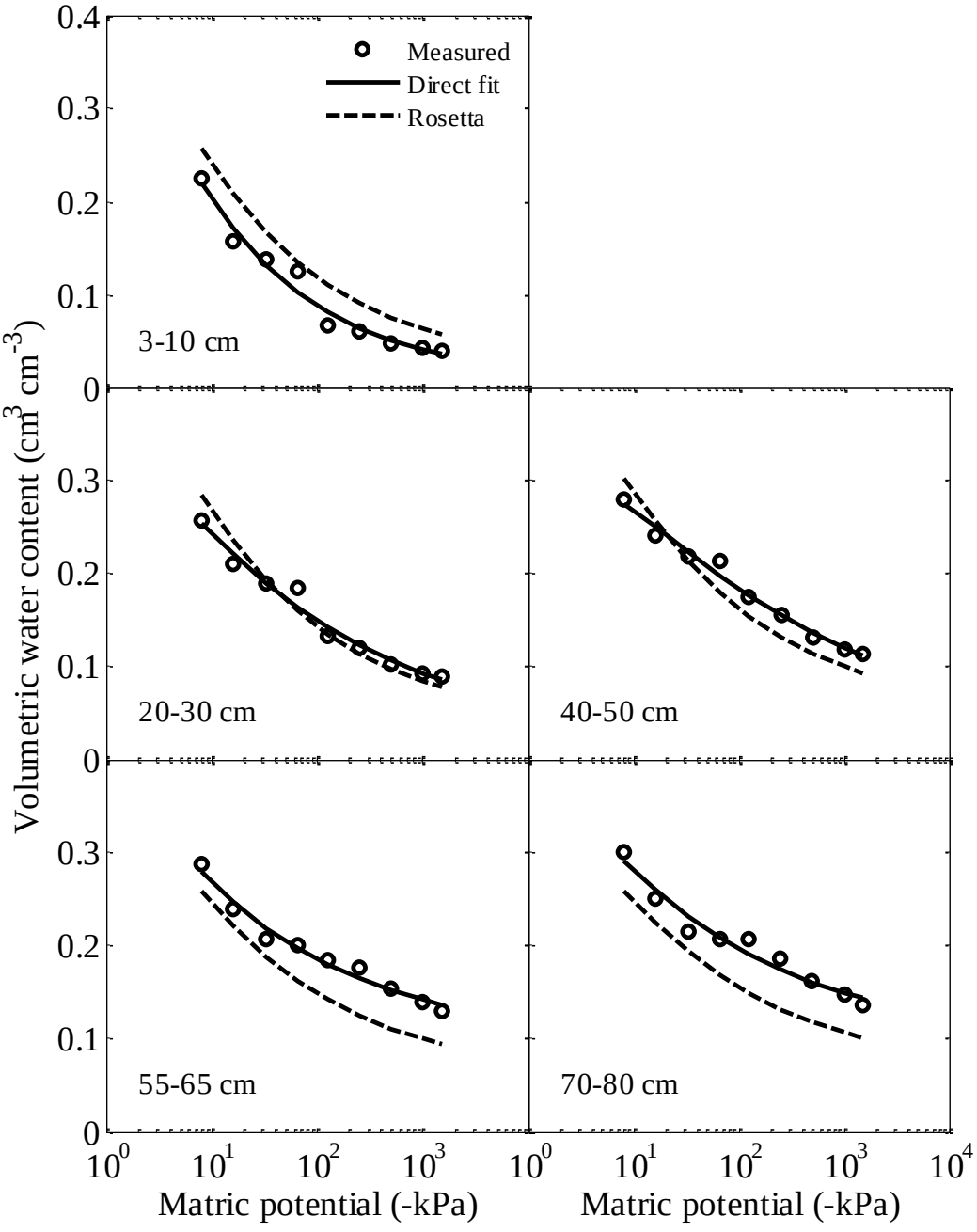

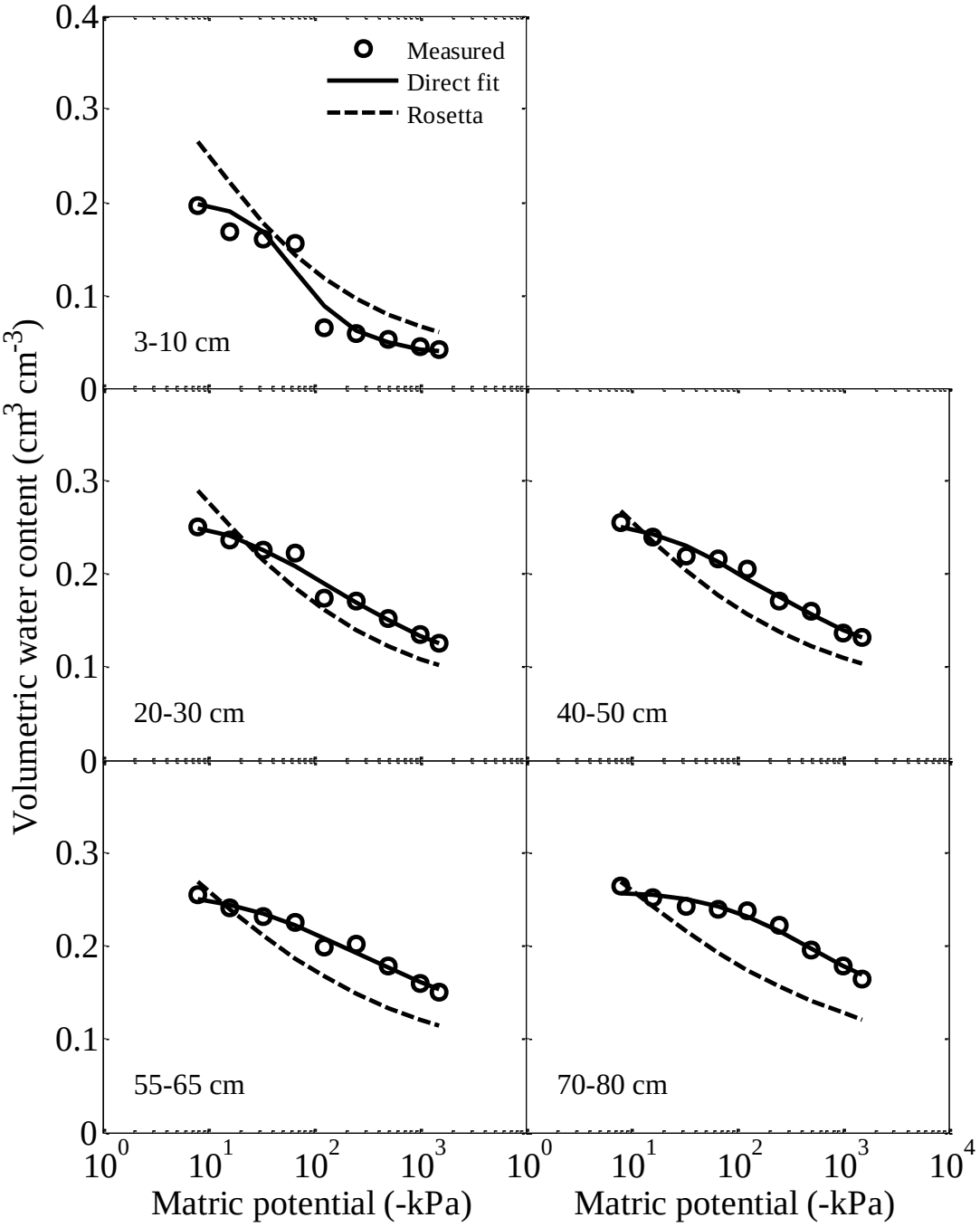
Measured
Direct fit
Rosetta
3-10 cm
20-30 cm
40-50 cm
55-65 cm
70-80 cm
Volumetric water content (cm3 cm-3)
Matric potential (-kPa)
Matric potential (-kPa)

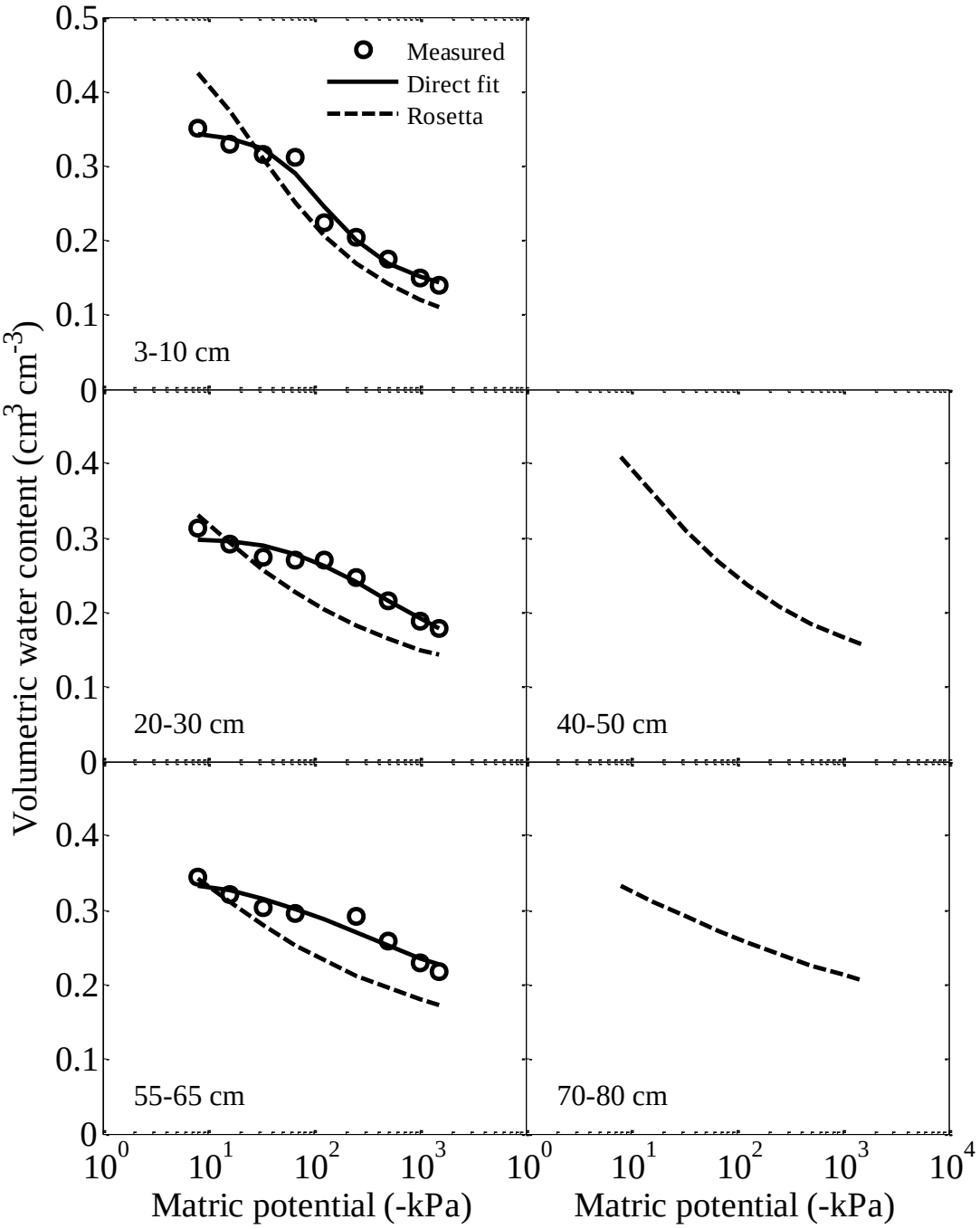
Measured
Direct fit
Rosetta
3-10 cm
20-30 cm
40-50 cm
55-65 cm
70-80 cm
Volumetric water content (cm3 cm-3)
Matric potential (-kPa)
Matric potential (-kPa)
0
0.1
0.2
0.3
0.4
0.5
10^0
10^1
10^2
10^3
10^4

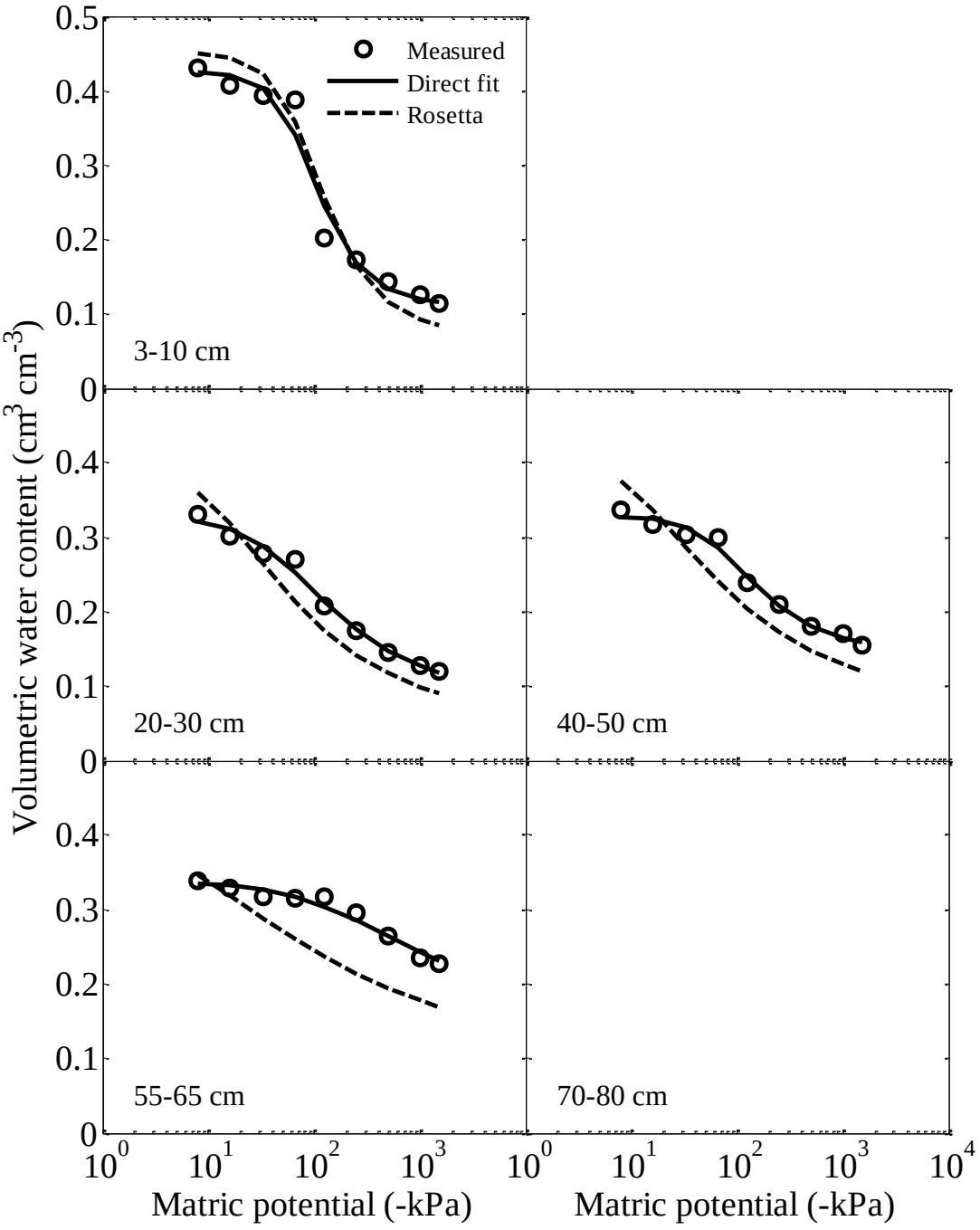
Measured
Direct fit
Rosetta
3-10 cm
20-30 cm
40-50 cm
55-65 cm
70-80 cm
Volumetric water content (cm3 cm-3)
Matric potential (-kPa)
Matric potential (-kPa)

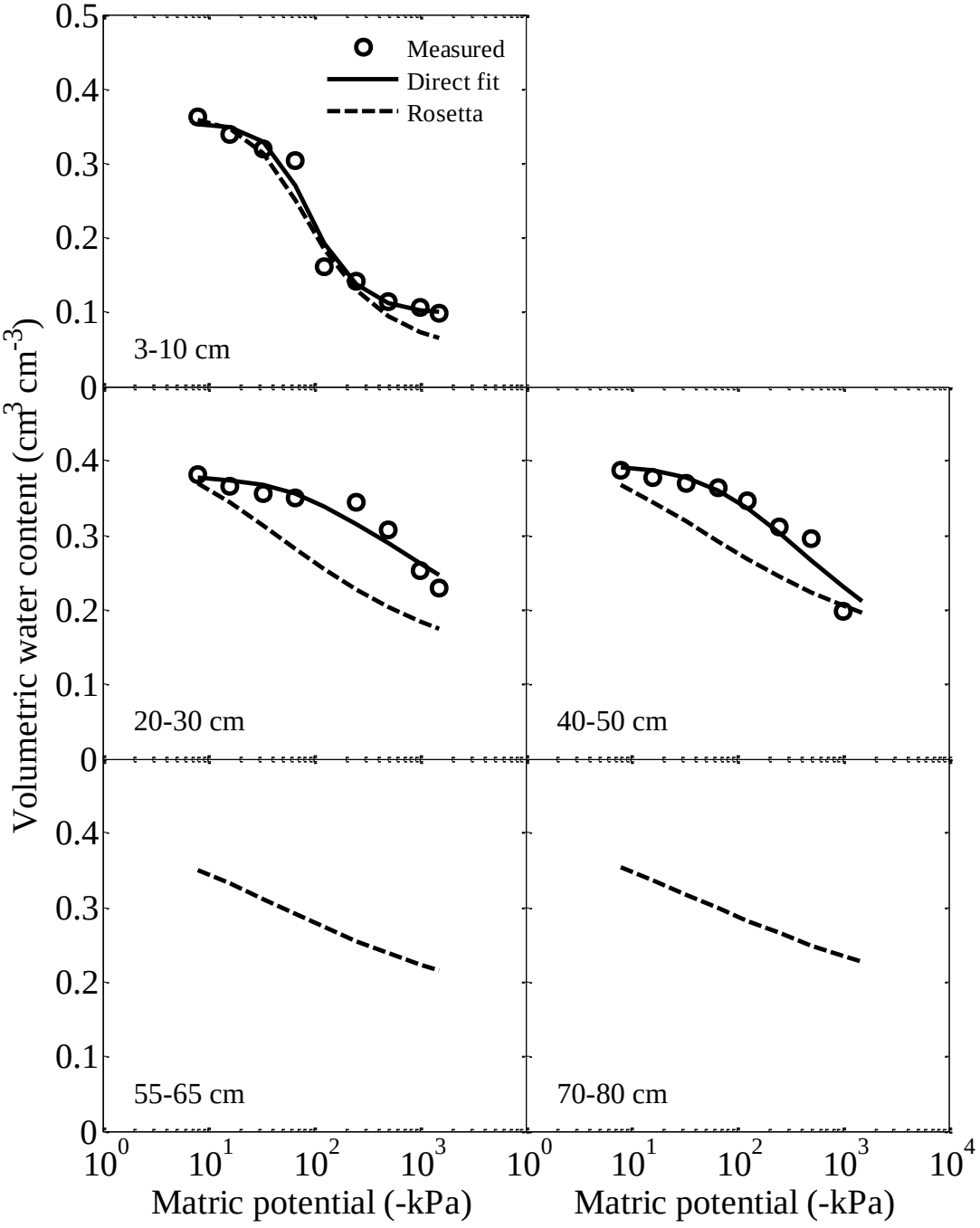
Measured
Direct fit
Rosetta
3-10 cm
20-30 cm
40-50 cm
55-65 cm
70-80 cm
Volumetric water content (cm3 cm-3)
Matric potential (-kPa)
Matric potential (-kPa)

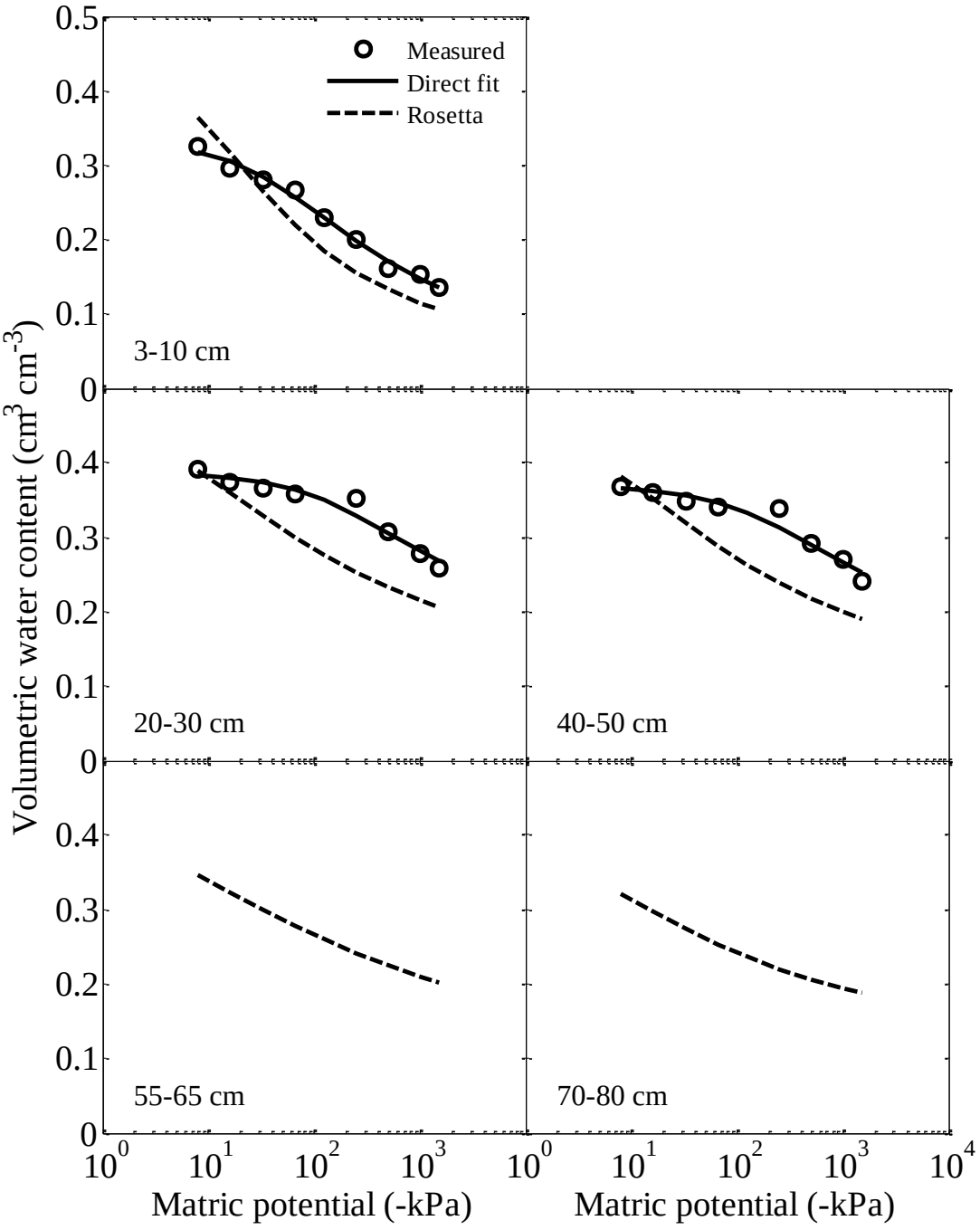
Measured
Direct fit
Rosetta
3-10 cm
20-30 cm
40-50 cm
55-65 cm
70-80 cm
Volumetric water content (cm3 cm-3)
Matric potential (-kPa)
Matric potential (-kPa)

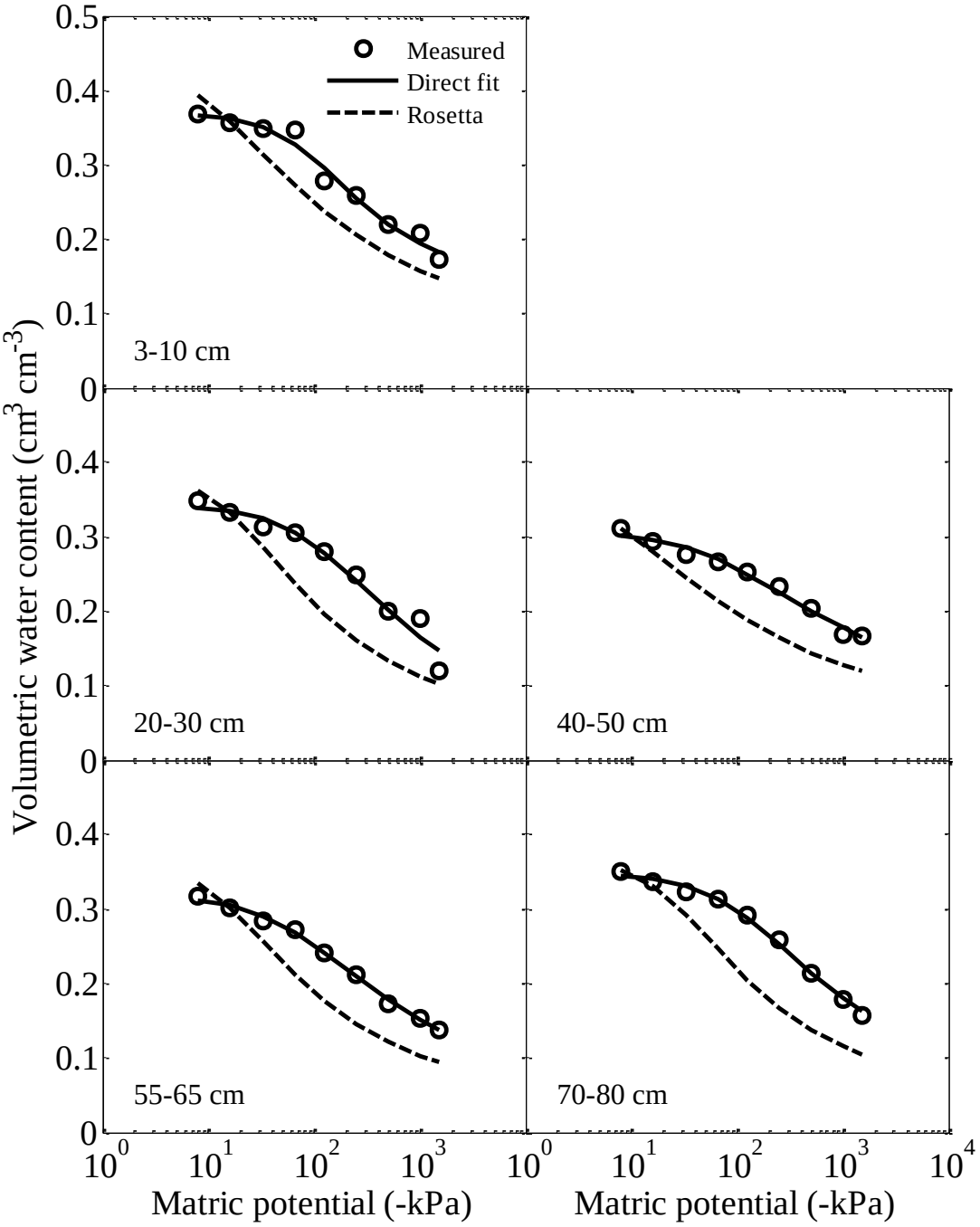
Measured
Direct fit
Rosetta
3-10 cm
20-30 cm
40-50 cm
55-65 cm
70-80 cm
Volumetric water content (cm3 cm-3)
Matric potential (-kPa)
Matric potential (-kPa)

APPENDIX II

The Matlab code used in processing the data for this thesis will be submitted electronically as a companion to this thesis. Created as part of the analysis, and to facilitate future analysis, the two Matlab function, MesothetaS and MesothetaT were created and are available for download at www.soilphysics.okstate.edu

VITA

Bethany Layne Scott

Candidate for the Degree of

Master of Science

Thesis: DEVELOPING A SOIL PROPERTY DATABASE FOR THE OKLAHOMA MESONET

Major Field: Plant and Soil Science

Biographical:

Education:

Completed the requirements for the Master of Science in Plant and Soil Science at Oklahoma State University, Stillwater, Oklahoma in December, 2012.

Completed the requirements for the Bachelor of Science in Environmental Science at Oklahoma State University, Stillwater, Oklahoma in May, 2010.

Experience:

Research Assistant, Dept. of Plant and Soil Sciences, Oklahoma State University, August, 2010 – July, 2012

Undergraduate Research Assistant, Dept. of Plant and Soil Sciences, Oklahoma State University, 2009-2010

Geographic Information Systems Intern, Bureau of Land Management, U.S. Department of the Interior, Summer 2009

Professional Memberships:

Soil Science Society of America, 2011

Agronomy Society of America, 2011

American Geophysical Union, 2010

Name: Bethany Scott Date of Degree: December, 2012

Institution: Oklahoma State University Location: Stillwater, Oklahoma

Title of Study: DEVELOPING A SOIL PROPERTY DATABASE FOR THE OKLAHOMA MESONET

Pages in Study: 63 Candidate for the Degree of Master of Science

Major Field: Plant and Soil Science

Scope and Method of Study: The objective of this study was to create a comprehensive database of soil hydraulic and physical properties of the Oklahoma Mesonet station soils. Replicate soil cores were collected at 117 Mesonet stations. The artificial neural network model Rosetta was used to estimate the van Genuchten water retention curve parameters, replacing the Arya and Paris estimated parameters.

Findings and Conclusions: The resulting database covers 13 environmental variables with 541 complete replicated sample sets that represent combinations of site and depth for 117 Mesonet Stations. The database contains the percent sand, silt, and clay; the bulk density, the volumetric water content at -33, and -1500 kPa; the van Genuchten parameters of residual volumetric water content, θ_r, saturated volumetric water content, θ_s ($cm^3\ cm^{-3}$), alpha, α (kpa^{-1}), and n (unitless); the saturated hydraulic conductivity, K_s ($cm\ day^{-1}$), as well as the matching point parameter, K_o ($cm\ day^{-1}$), and the empirical parameter, L (unitless). The performance of the Rosetta model was determined based on the root mean squared difference (RMSD) of the modeled data vs. that found through oven-drying and was found to be 0.053 $cm^3\ cm^{-3}$, compared to the Arya and Paris method RMSD of 0.078 $cm^3\ cm^{-3}$. The improved estimates of the soil hydraulic and physical properties of the Mesonet station soils has expanded the functionality of the monitoring system by providing increased accuracy for the Mesonet soil water content data. The estimation of soil water content by the Oklahoma Mesonet was improved by 32%. In addition, daily plant available water maps are currently available on the website, www.mesonet.org.

ADVISER'S APPROVAL: Dr. Tyson Ochsner